OPTIMISATION OF BIOLEACHING OF MALAYSIAN AND CHINESE KAOLIN

LEE WEI SHEONG

UNIVERSITI TUNKU ABDUL RAHMAN

OPTIMISATION OF BIOLEACHING OF MALAYSIAN AND CHINESE KAOLIN

LEE WEI SHEONG

A project report submitted in partial fulfilment of the requirements for the award of Bachelor of Mechanical Engineering with Honours

Lee Kong Chian Faculty of Engineering and Science
Universiti Tunku Abdul Rahman

May 2023

DECLARATION

I hereby declare that this project report is based on my original work except for citations and quotations which have been duly acknowledged. I also declare that it has not been previously and concurrently submitted for any other degree or award at UTAR or other institutions.

Signature : 

Name : Lee Wei Sheong

ID No. : 1804847

Date : 26 April 2023

APPROVAL FOR SUBMISSION

I certify that this project report entitled **"OPTIMISATION OF BIOLEACHING OF MALAYSIAN AND CHINESE KAOLIN"** was prepared by **LEE WEI SHEONG** has met the required standard for submission in partial fulfilment of the requirements for the award of Bachelor of Mechanical Engineering with Honours at Universiti Tunku Abdul Rahman.

Approved by,

Signature : 

Supervisor : Dr. Kuan Seng How

Date : 28 April 2023

Signature :

Co-Supervisor :

Date :

ACKNOWLEDGEMENTS

I would like to thank everyone who had contributed to the successful completion of this project. I would like to express my gratitude to my research supervisor, Dr. Kuan Seng How for his invaluable advice, guidance and his enormous patience throughout the development of the research.

In addition, I would also like to express my gratitude to my loving parents and friends who had helped and given me encouragement to conduct this project. I would also like to thank my senior Yong Shih Nee who guided me in conducting the experiments, and facilities provided by Universiti Kebangsaan Malaysia.

ABSTRACT

Kaolin has impurities such as iron which led to reduced quality, brightness and viability in industrial applications. Therefore, iron extraction was developed to increase the quality of kaolin. The bioleaching method could be an alternative to produce good quality kaolin as bacteria, being an organic compound is environmental friendly. But before bioleaching can be implemented as an alternative, it needs to be optimised to a feasible efficiency of at least 80 %. Hence, optimisation of bioleaching of kaolin is necessary. It was found that the optimum nutrients condition for bioleaching kaolin with *B. cereus* is 8 g/L of glucose concentration while for *B. megaterium* and *B. aryabhattai* the optimum glucose concentration is 10 g/L. Iron reduction ability of *Bacillus* bacteria was measured and reduction of iron was clearly visible in phenanthroline analysis and ICP-OES analysis whereby the Fe(II) concentration increased during the period of 10 days of bioleaching. The EDX analysis revealed that a slightly higher bioleaching efficiency was achieved as compared to the previous studies. Malaysian kaolin treated with *B. cereus*, *B. megaterium* and *B. aryabhattai* was found to be 57.4 %, 60.3 % and 65.9 % respectively. Whereas for Chinese kaolin treated with *B. cereus*, *B. megaterium* and *B. aryabhattai*, the bioleaching efficiency was found to be 41.6 %, 54.7 % and 62.8 % respectively. Optimum glucose concentration used for the bioleaching experiment could be the contributing factor to the small increase in the bioleaching efficiency. Malaysian and Chinese kaolin experienced changes in terms of structure and surface morphology after bioleaching with *Bacillus* spp. bacteria based on the SEM analysis. The surface structure of both Malaysian and Chinese kaolin changed from amorphous to a more crystalline structure while the chemical composition and bonds of both Malaysian and Chinese kaolin remains unchanged after bioleaching as determined in the XRD and FTIR analysis. The results showed improvements in the bioleaching efficiency, contributing to the studies of implementing bioleaching in the industrial scale. With more laboratory scale experiments of optimisation, bioleaching will be able to replace chemical leaching with a lower cost and sustain and protect the environment.

TABLE OF CONTENTS

LIST OF TABLES

LIST OF FIGURES

LIST OF SYMBOLS / ABBREVIATIONS

M	Molarity, mole/L
AQDS	9,10-anthraquinone-2,6-disulphonic acid
B.	Bacillus
CEC	Cation exchange capacity
cfu	Colony-forming unit
EDS	Energy-dispersive spectroscopy
EDTA	Ethylenediaminetetraacetic acid
EDX	Energy Dispersive X-Ray Spectroscopy
EPS	Extracellular polymeric substances
Fe	Iron
FTIR	Fourier Transformed Infrared Spectroscopy
ICP-OES	Inductively Coupled Plasma Optical Emission Spectroscopy
IRB	Iron-reducing bacteria
NTA	Nitrilotriacetic acid
ppm	Parts per million
SEM	Scanning Electron Microscopy
spp.	Species
XRD	X-Ray Diffraction

LIST OF APPENDICES

CHAPTER 1

INTRODUCTION

1.1 General Introduction

Kaolin is a type of clay naturally found on earth (Hubadillah, et al., 2018). Kaolinite, the dominant mineral in kaolin has the chemical formula of $Al_2(Si_2O_5)(OH)_4$ and has an uncharged dioctahedral layer structure of 1:1 whereby each layer has single alumina octahedral sheet and single silica tetrahedral sheet (Abdullahi, Harun and Othman, 2017). According to Murray (2006), it is estimated that some 40,000,000 tons are mined and processed annually. There are various applications that uses kaolin such as coating and filling of paper, pigments in paint, ceramics production, filler in plastics, fertilizers, detergent and production of fiberglass (Buyondo, Kasedde and Kirabira, 2022; Huang, et al., 2019).

However, there are impurities such as iron oxides found in kaolin which reduces the quality, brightness, refractions and viability of kaolin application. Iron oxides or iron hydroxides impart red to yellow color onto the kaolin. The quality of non-metallic raw materials was decreased by iron minerals (Štyriaková, et al., 2010). There is certain standard of iron content in kaolin to be met in the industry because iron-bearing impurities affects the commercial value of kaolin raw materials, due to the detrimental effect on the refractoriness and whiteness of products manufactured from kaolin that contains iron impurities (Zegeye, et al., 2013). For example, the kaolin used in fiberglass production must meet stringent chemical specification of maximum 0.6 % Fe_2O_3 (Murray, 2006), kaolin with 0.48 % of Fe_2O_3 will be able to fit for applications in paper, plastic and rubber industries (Gougazeh, 2018). Therefore, many physical, chemical and biological methods have been developed to extract iron from raw kaolin in the recent decades.

Physical method refers to magnetic separation and gravity separation while chemical methods uses chemicals such as acids and alkaline and strong chemical reducers to leach kaolin which can extract up to 80 % to 98 % of iron from kaolin (Hernández, et al., 2013). However, chemical leaching requires high cost of storage and transport and cause environmental harm (Fakharpour

and Hajihoseini, 2021). Furthermore, chemical leaching becomes impractical when large amount of kaolin need to be leached as a large amount of reagent will need to be used. There is a lower efficiency by physical method as iron in kaolin may exist in complex form. Hence, bioleaching has been studied by previous researchers to overcome the disadvantages of both physical and chemical means of iron extraction from kaolin. Bioleaching method is more economical and environmental friendly in extracting iron from kaolin (Wang, et al., 2017; Roy, et al., 2021; Kaksonen, et al., 2018) but it has a lower efficiency. Therefore, optimisation of bioleaching of kaolin will be investigated in this study.

1.2 Importance of the Study

This study may provide the optimization of the bioleaching process of the *Bacillus* species bacteria. The effectiveness of the *Bacillus* bacteria and its optimum condition for bioleaching may provide a solution to a higher extraction of iron from kaolin or valuable insight for further research on *Bacillus* bacteria bioleaching. This will result in a better quality kaolin from bioleaching to be used in different industrial applications. The bioleaching method may become an alternative to produce good quality kaolin as organic compound such as bacteria is environmental friendly (Hernández, et al., 2013).

It is necessary to provide research results based the increased in quality of kaolin to add value to the bioleaching method, therefore this report presents the investigation of iron extraction from kaolin clay through bioleaching to obtain the optimum experimental conditions for future implementations of bioleaching in the industry.

1.3 Problem Statement

Low iron composition kaolin is highly demanded, which led to high quality kaolin on verge of being exhausted (Lee, Cho and Ryu, 2002). Extraction of iron from kaolin brings better commercial value of kaolin but physical methods and chemical methods of extracting iron from kaolin has not meet the cost and efficiency requirements of the industry. The chemical leaching of kaolin produces a kaolin with approximately 2 wt.% of iron(III) oxide, which is still far from required commercial quality (Sanchez-Palencia, et al., 2022).

Even though bioleaching has been studied by previous researchers, it is not optimised to be use in a large scale in the industries. The bioleaching of kaolin takes longer time than other methods which makes it not suitable in various industries. This is because in the manufacturing and fabrication industry, time is one of the main concern of production. A higher production yield in a short time may increase the commercial revenue in the industry. This project aims to address this issue by bringing bioleaching a step closer to be implemented in the industry through improving the bioleaching efficiency. While there are many parameters that could be optimised, this project focus on the optimisation of nutrients concentration as it was not done in detailed research in previous studies. Due to time and resources limitation, the other parameters that could be optimised are listed in Chapter 3 for further studies. The inconsistent amount of iron extracted through bioleaching has not been clarified in detail in previous studies. Hence, some of the mechanisms of bioleaching will be discussed in the literature review of this report and the optimum nutrient condition for bioleaching will be investigated.

In some of the previous works, the kaolin samples were not sterilized prior to the experiments, so any influence of natural microbiota was not taken into account (Sanchez-Palencia, et al., 2022). Therefore, in this experiment the transfer of sub-culture and equipment are done in condition to avoid contamination such as using the aseptic technique.

Although bacterial species showed that high quality of kaolin may be produced in certain experimental method described in the literature, a recent study by Sanchez-Palencia, et al. (2022) leached only 0.83 % of iron. Thus, in order to develop a method with consistent and high efficiency leaching of iron, more attempts and research is needed.

1.4 Aim and Objectives

The objective of this study is to optimise the bioleaching of Malaysian and Chinese kaolin through:

(i) Determine the optimum nutrients concentration for bioleaching.

(ii) Measure and compare the iron reduction ability of *Bacillus cereus*, *Bacillus megaterium* and *Bacillus aryabhattai* in

Malaysian and Chinese kaolin using phenanthroline, EDX and ICP-OES analysis.

(iii) Determine the morphological and structural changes of kaolin particles during bioleaching through SEM, FTIR and XRD analysis.

1.5 Scope and Limitation of the Study

This research focus on optimization of bioleaching to enhance quality of kaolin, in terms of colour properties by leaching Fe(III) iron impurities from Malaysian and Chinese kaolin. Morphological analysis was carried out on the kaolin before and after bioleaching as described in Chapter 3. *Bacillus* spp. bacteria are easily available in the nature, an average of 1.9 % of *Bacillus* was detected in soil with and relative increase of 3.2 % in the dump soil (Puglisi, et al., 2019). *Bacillus* has a relative abundance of 6 % in garden soils and 5 % in saline soils. *Bacillus* is particularly predominant in the sludge, due to their their ability to resist desiccation that ultimately increase their abundance (Mhete, et al., 2020). Hence, *Bacillus* sp. was used in previous studies and the amount of iron impurities extracted from previous studies will be able to be compared with the current study to optimise the bioleaching of Malaysian and Chinese kaolin.

Limitation of the study is the amount of Fe(III) impurities differs from kaolin to kaolin, it varies based on the deposit origin and geological processes (Zegeye, et al., 2013). Since the kaolin used in this study is from different origin which is Malaysian kaolin and Chinese kaolin, the comparison of the bioleaching process between the two different origin kaolin may not reflect on other kaolin.

Furthermore, there are others bacteria that might be more effective than *Bacillus cereus*, *Bacillus megaterium* and *Bacillus aryabhattai*. However, due to the limited resources, only these three bacteria will be investigated in this study.

1.6 Contribution of the Study

This study contributes to the sustainability of environment by reducing chemical waste and investigate the viability of replacing the extraction of iron

from kaolin by bioleaching method. A study also suggest that the acidic waste generated from chemical leaching process brings harm to the natural environment (Ribeiro, et al., 2007). In the European Union and many other places, kaolin waste dumps represent an environmental and economic problem because of the presence of iron minerals as contaminants within the kaolin that cause them to be commercially unviable (Sanchez-Palencia, et al., 2022). The bioleaching of kaolin using *Bacillus* bacteria also aligns with conserving and sustaining the life below water in Sustainable Development Goals (SDGs) as the chemical waste from chemical leaching will pollute and endanger organisms in lakes and rivers.

This study also provides the ability of *Bacillus* species bacteria to leach iron as an alternative with lower cost compared to the conventional method. This study may also contribute to the study of leaching mechanism in future research since the mechanism can allow us to adjust when the bacteria bind to the iron impurities in kaolin and hence allow us to control the leaching time.

1.7 Outline of the Report

This report consists of five chapters, Chapter 1 discuss the introduction and background, importance of study, problem statement, aim and objectives, scope and limitations along with contribution of the study to provide basic understanding of bioleaching, the need for alternatives to conventional iron leaching methods and the benefits of bioleaching to environment.

Chapter 2 is the literature reviews which covers the literature reviews of the previous research and provide a basis for the study and experiments. The factors and ways to optimise bioleaching as well as the methods involved in bioleaching were discussed.

Chapter 3 explains the methodology of the experiment with the flow of the experiment, chemicals and materials required and their usage. Equipment and the required settings for the experiments are also stated.

Chapter 4 presents the findings and discussion of the results from the various analysis conducted. The results are also compared with the previous studies to provide readers with a clearer understanding.

Lastly, Chapter 5 concludes the findings from the experiments and recommendation for future work.

CHAPTER 2

LITERATURE REVIEW

2.1 Introduction

There are different methods of extracting iron (Fe) from kaolin such as chemical leaching and magnetic separation before bioleaching is being studied as an alternative to the conventional methods.

Chemical leaching refers to the extraction using acids or alkaline and potent reducers in reductive leaching, for example sodium dithionite plus aluminum sulphate, hydroxyl ammonium acid sulphate. The composition of kaolin changed considerably after the acid treatment (Kumar, Panda and Singh, 2013). The chemical leaching improved the brightness to an average of 85.6. There is a high percentage of iron-oxide removal and produce a kaolin containing 0.48% Fe_2O_3, which satisfy the industrial's applications standard. After reducing the Fe_2O_3 contents with sodium hydrosulphite (dithionite, $Na_2S_2O_4$) by using the chemical leaching, it is obvious that iron oxides are not present in the pattern obtained as compared to the peaks representing Fe_2O_3 that the X-Ray Diffraction (XRD) pattern obtained for untreated samples (Gougazeh, 2018).

Chemical leaching alters the composition of kaolin, affecting the properties of kaolin (Hosseini, et al., 2007). Serious environmental threat was pointed out on the chemical leaching method and may become serious during rainy season (Hussain, et al., 2013). In chemical leaching, the chemical waste has to be well handled to avoid any harm to the environment. An alternative to the chemical leaching would be better as it completely removes the possibility of having harmful chemical waste from extraction of Fe from kaolin.

Other than chemical leaching method, magnetic separation is also one of the Fe extraction method. White color and high quality of raw materials could be achieved through biological leaching of Fe and subsequent electromagnetic separation (Štyriaková, Štyriak, Malachovský and Lovás, 2006). By adding electromagnetic separation after bioleaching, the 0.13 % iron oxide content of the quartz sand decreased to 0.02 % (Štyriaková, et al., 2007). Magnetic separation can remove iron-bearing minerals but disadvantage of

conventional mineral processing methods is ultra-fine Fe particles are difficult to treat (Štyriaková, Štyriak and Malachovský, 2007). On top of that, electromagnetic separation will require continuous supply of electricity and if permanent magnet is used, replacement of the magnet is costly. A previous study also reported that the amount of Fe mineral in high gradient magnetic separated kaolin has not met the required paper industry Fe grade (Tahli, 2008). Therefore, bioleaching is a better alternative for the extraction of Fe from kaolin.

This chapter covers the literature review on bioleaching of kaolin as well as the effects after kaolin is leached. Besides, the two different method of bioleaching which are in-situ and two stage bioleaching is also covered in this chapter. Lastly, the ways to enhance the bioleaching process is reviewed at the last part of the chapter.

2.2 Bioleaching of kaolin

The red color of kaolin becomes more prominent as the iron oxide amount increases, resulting in the reduction of the refractory property and lead to the cracks formation during firing caused by impurities (Arslan and Bayat, 2009). The most important factor to determine the quality of the clay is, therefore, the color of kaolin as whiteness of the clay classify the quality of kaolin. There are various methods to improve the quality of kaolin by extracting Fe impurities from natural kaolin. These methods include froth floatation, gravity separation, bioleaching, chemical leaching and magnetic separation to separate Fe from kaolinite (Guo, Lin, Xu and Chen, 2010). The method of bioleaching is environmental friendly and relatively low cost. Colour analyses of the bioleached kaolin showed that after five days of incubation at 30 °C, there is a remarkable increase in brightness and whiteness compared to the untreated kaolin (Zegeye, et al., 2013). Hence, bioleaching of kaolin becomes the main alternative to the conventional way of Fe extraction from kaolin using chemicals.

Bioleaching of kaolin refers to the extraction of Fe impurities from kaolin using microorganism such as iron-reducing bacteria (IRB) or fungi. There is no secondary mineral phase formation and structural changes when Fe was selectively leached from kaolin, but there was improvement in terms of

the structure crystallinity (Guo, Lin, Xu and Chen, 2010). Fungus is able to leach Fe through the organic acid excretion. However, toxins are often produced from fungus which could be a risk factor of technological process and products quality might be affected (Štyriaková, Štyriak and Kušnierová, 1999). Therefore, fungus is not preferred in the industry.

There are various bacteria discovered to be able to leach Fe from kaolin. X-Ray analysis confirmed the biodegradation ability of the bacterial strains and the removal of individual metal cations from the samples was determined by atomic absorption spectrometry (Štyriaková, Štyriak and Kušnierová, 1999). Yap, et al. (2020) found that Fe (III) oxide impurities present in kaolin could be reduced by *Bacillus cereus*. In another study by Štyriaková, Štyriak, Nandakumar and Mattiasson (2003), *B. cereus* growth and metabolic activities after 3 months of bioleaching were found to extract 49 % Fe from the kaolin sample in the octahedral position in mica and 17 % in the quartz sands sample. Selim and Rostom (2017) discovered *B. cereus* bacterial strain selectively separates hematite from its mixture with silica as a sole flocculating agent, it successfully removed 98 % of Fe_2O_3 with 82 % flocculated by weight and recovery of 89.20%. Bioleaching with *Bacillus* spp. bacteria removed 60% of the Fe content in quartz sands (Štyriaková, et al., 2007) as *Bacillus* spp. are effective secretors of metabolites (Abdel-Shafi, Reda and Ismail, 2017). Arslan and Bayat (2009) also found that 77.13% of the total Fe was removed from the result of bioleaching of kaolin by *Aspergillus niger*, suggesting that this strain is effective at removing Fe impurities from kaolin. Another study showed that after 1 month of bioleaching, bacteria of *Bacillus* species are able to leach 43 % of free Fe in kaolin in amorphous form of oxyhydroxides and approximately 15 % of bound Fe in mica (Štyriaková and Štyriak, 2000). In a study by Zegeye, et al. (2013), all tested IRB of the *Shewanella sp*. bacterial strains were able to improve the color properties of kaolin by reducing and leaching of ferric iron present in the industrial kaolin.

Growing heterotrophic bacteria are able to dissolve Fe in feldspar raw materials (Štyriaková, Štyriak, Malachovský and Lovás, 2006). The bioleaching of quartz sand dissolve coating of Fe(III) impurities on quartz grains surface (Štyriaková, et al., 2010). It was suggested that the biological

and chemical destruction of quartz after bacterial leaching was more effective than chemical leaching (Štyriaková, Štyriak and Kušnierová, 1999).

2.3 Effects of Bioleaching

Micro-organisms leached out insoluble Fe(III) as water-soluble Fe(II) as shown in Equation 2.1, either adsorbed to the kaolin surfaces or admixed as amorphous forms (Guo, et al., 2010). The leached Fe(II) are found in the medium and identified through experimental methods such as the Phenanthroline method.

$$Fe^{3+} \text{ (Ferric ion)} + e^- \rightarrow Fe^{2+} \text{ (Ferrous iron, aq)} \quad (2.1)$$

Some of the studies observed that there is alteration of surface chemistry of minerals results of adhesion of microorganisms to minerals (Abdel-Khalek, et al., 2013). Kaolin undergone textural and mineralogical changes, resulted in a decrease in kaolin particle size after bioleaching (Guo, et al., 2010). A granulometric analysis of dispersed kaolin showed that the bioleaching resulted in reduced particle size (Guo, et al., 2010). A similar result was obtained by Štyriaková, et al. (2012) showing that after bioleaching, the finest fraction was destructed in grain size analyses.

Štyriaková, Štyriak, Nandakumar and Mattiasson (2003) also found a different morphology before and after bioleaching in the boundary region of mica grains, there was presence of silica indicating silicate destruction during bioleaching (Štyriaková, Štyriak, Malachovský and Lovás, 2006). After bioleaching, calcium oxalate dehydrates (weddellite) was identified as a new mineral, found within the fine grain fraction of samples as shown in Figure 2.1 represented by ‘W’ (Štyriaková, Štyriak, Malachovský and Lovás, 2006). X-ray analysis by Štyriaková and Štyriak (2000) confirmed the iron oxyhydroxides biodegradation and partial structure destruction of mica. Štyriaková, Štyriak and Kušnierová (1999) confirmed morphological changes by the ability of bacteria to destroy some silicates and to produce the release of several metal cations from their structure.

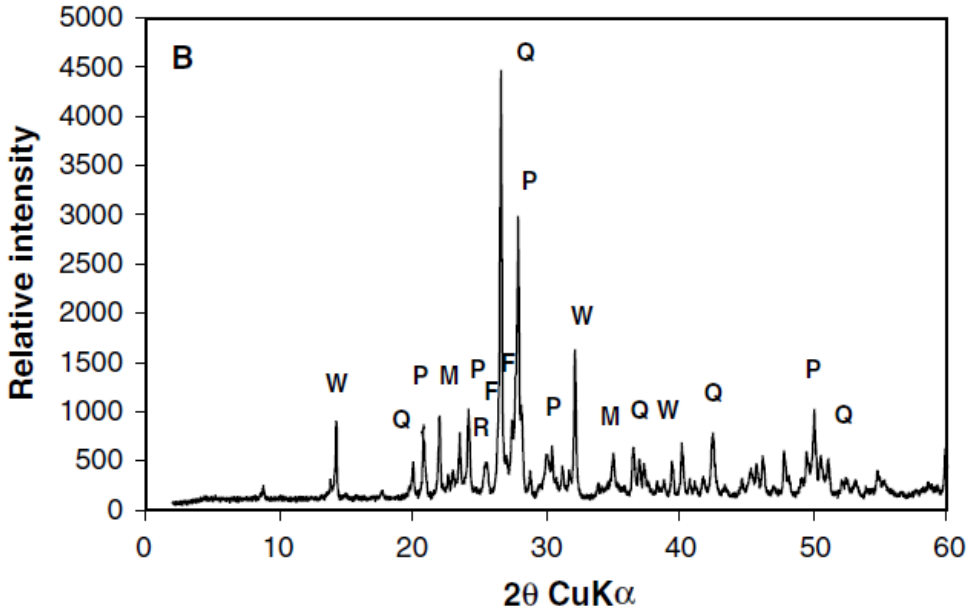

Figure 2.1: X-ray Diffraction Spectrum After bioleaching (Štyriaková, Štyriak, Malachovský and Lovás, 2006).

However, some studies found that there is no new band in Fourier Transform Infrared spectroscopy (FTIR) of the kaolin sample after bioleaching as shown in Figure 2.2, suggesting that the structural composition has no major change (He, Huang and Chen, 2011).

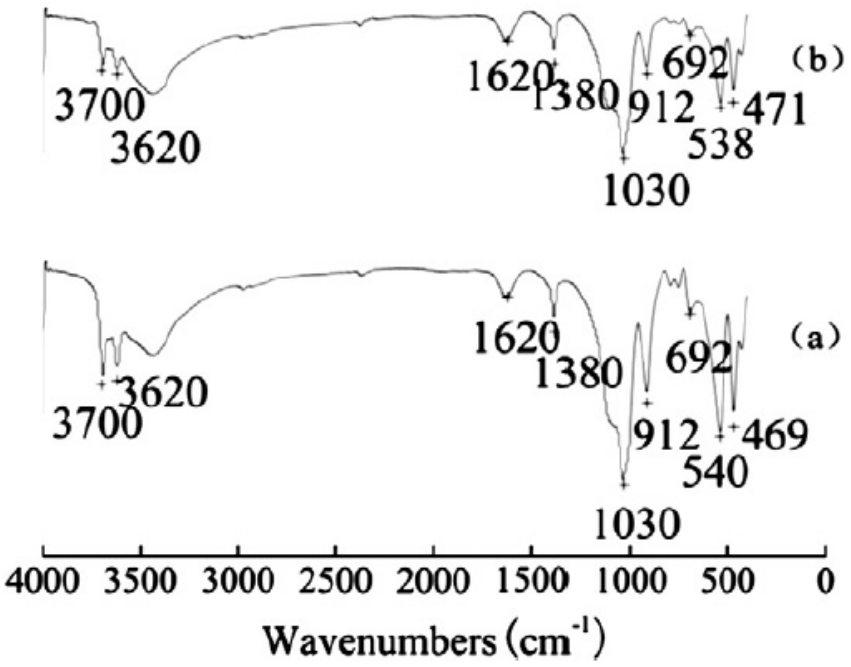

Figure 2.2: Spectrum of FTIR analysis (a) Before Bioleaching and (b) After bioleaching (He, Huang and Chen, 2011).

Moreover, Guo, Lin, Xu and Chen (2010) also observed that there are no significant changes of either the structure or major mineral compositions from microbial refinement, but the degree of crystallinity did improve. Kaolin samples that were more amorphous in structure are transformed to a more crystalline structure and formed finer particles after bioleaching (Guo, Lin, Xu and Chen, 2010). Zegeye, et al. (2013) suggest that XRD and infrared spectroscopy shows neither crystal-chemical alteration nor secondary mineral, Energy-dispersive spectroscopy (EDS) analysis indicated that there is no significant chemical composition change in the kaolin after bioleaching.

Although there is no mineralogical or chemical alteration, it was observed that the initial hexagon shape of the biotreated kaolin particles became less regular as compared to the original particles, indicating that the particles became more crystalline from an amorphous structure. A recent study supports this observation as shown in Figure 2.3, the structures of the untreated kaolin particles are more amorphous. However, in Figure 2.4 the SEM image revealed that the structure is more crystalline after bioleaching. The particles specific surface area also decreased as compared to the original sample after the samples are treated with bacteria of *Bacillus* spp. that produces organic acids and indigenous heterotrophic bacteria (Štyriaková, et al., 2012).

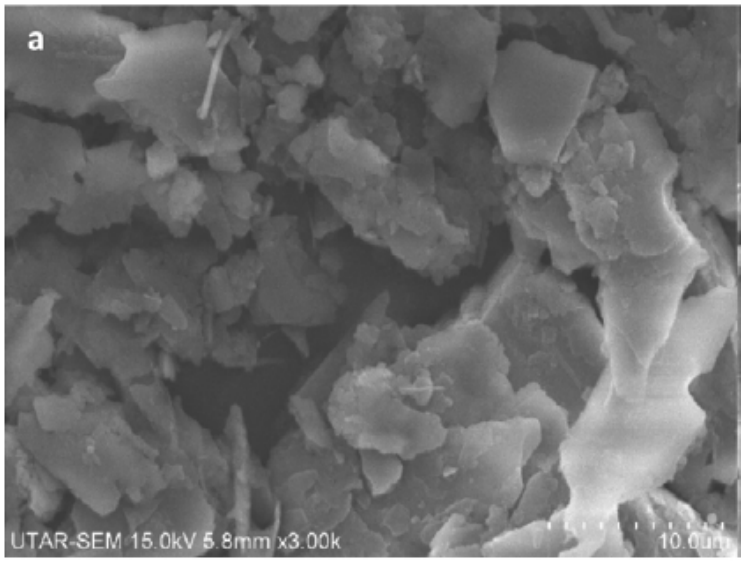

Figure 2.3: SEM image of Kaolin Particles Before Bioleaching (Yap, et al., 2020).

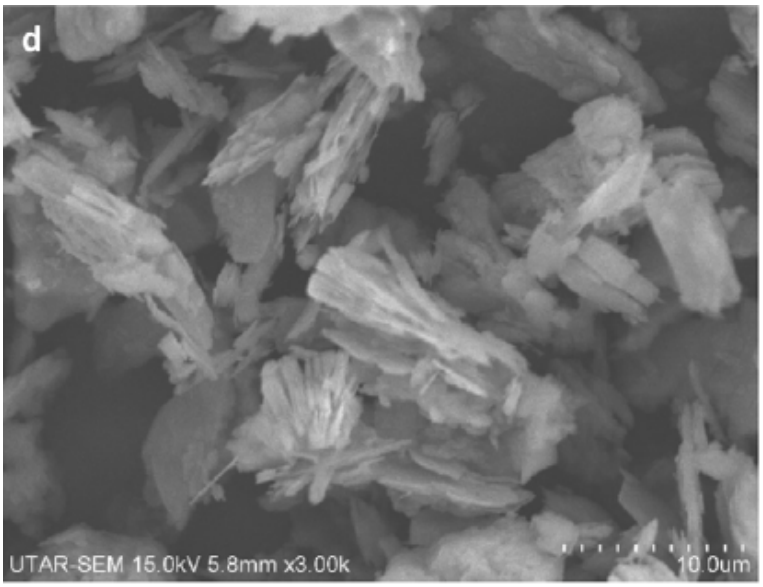

Figure 2.4: SEM image of Kaolin Particles After Bioleaching (Yap, et al., 2020).

After the Fe impurities are removed, mica with phengite composition are biologically destructed and led to the development of illite, illite development enriched the kaolin sample by fine-grained fraction (Štyriaková, Štyriak, Nandakumar and Mattiasson, 2003). The silica particles were more dispersed in the pulp as a degree of aggregation for iron oxide surface was caused by successful adsorption of *B. cereus* (Selim and Rostom, 2017).

2.4 Techniques of bioleaching

The bioleaching of kaolin is generally conducted in two different ways. First is the "in-situ" technique whereby the process of microbial growth and bioleaching is done simultaneously in which the metabolism of microorganisms occurs in the presence of clay. Nevertheless, microbial fermentation is first carried out in the two-stage bioleaching method, followed by clay bioleaching stage that is performed using the separated metabolites from the bacteria cells.

2.4.1 In-situ Bioleaching Method

According to Cameselle, et al. (2003), "In situ" leaching technique is dependent on the bacteria and bacterial strain used. There is a lower Fe removal by *A. niger* CBS 246-65 strain, but strain 1120 leached Fe efficiently.

This is due to strain 1120 has a greater capacity to produce oxalic acid as compared with CBS 246-65.

Addition of carbon source to the mineral to grow the selected strain or strains could bioleach heavy metal by “in-situ method”. Microorganism cultivation take place together with the leaching of heavy metal for in-situ method. This technique could be performed easily, but the microorganism metabolism and growth may be affected by the dissolved metal ions, limiting the efficiency of bioleaching process. Moreover, there may be different optimum operating conditions for leaching and culture (Cameselle, et al., 2003). A previous study came to the conclusion that “in-situ” leaching has many disadvantages which make this technique not suitable for large scale bioleaching (Cameselle, et al., 2003). The Fe dissolution rate of in-situ leaching is lower when compared to the two-stage technique, changing any other variables or performing the process at higher temperature may improve it but will cause damage to the microorganism.

2.4.2 Two Stage Bioleaching Method

As an alternative to overcome the drawbacks of the “in-situ” method, the bioleaching may be conducted in two stages. In this case, the cultivation of the bacteria and bioleaching are performed at their optimum working conditions separately. In the first stage, the microorganism should be grown with a substrate, nitrogen and phosphorus sources enriched medium under suitable culture conditions to increase the active production and maximise the acid production as preparation for the second stage leaching process. Jing, et al. (2021) found that in their research study, out of the five microbes they investigated under nitrogen-rich condition, *Bacillus cereus* and *Staphylococcus aureus* outperformed other microbes. During the second stage of the bioleaching process, spent culture medium will then be used as the leaching agent of the mineral (Cameselle, et al., 2003).

The implementation of more a vigorous leaching conditions such as lower pH and optimum temperature for bioleaching are permitted in the absence of a growing microorganism during the second stage (Arslan, 2021), therefore acquired a higher dissolution rate and extent of Fe removal. Because

the organic oxalic acid in the sample is only active at about pH 2, the higher the pH value, the lower the activity of oxalic acid (Cameselle, et al., 2003).

2.5 Factors Affecting Bioleaching

There are various factors that affects the efficiency of bioleaching of kaolin. Many studies including a study by Jing, et al. (2021) suggest that iron-reducing ability of a microorganism to dissolve ferric(III) oxide in the kaolin is attributed to its organic acids production. A reducing environment was expected as a result of the bacterial metabolic activities which could generate organic acids (Sanchez-Palencia, et al., 2022). Studies by Hosseini and Ahmadi (2015) concluded that oxalic acid was much more effective and capable of removing and complexing Fe than citric acids. Saeid, et al. (2018) outlined that gluconic, acetic, lactic, succinic and propionic acids were produced by *B. cereus* and *B. subtilis* in which lactic and acetic acids has the highest amount. It is the same for *B. megaterium* with an exception of not producing propionic acid. The Fe contained in minerals are solubilized by organic acids that were produced by *Bacillus* spp. thus reducing the impurities in clay minerals (Yong, et al., 2022). A similar result was observed in a study by Arslan and Bayat (2009); He, Huang and Chen (2011) whereby the Fe impurities removal were increased with the presence of oxalic acid in the leaching medium.

Besides, the higher cell concentration will result in a higher removal of Fe(III) as shown in Figure 2.5, the concentration of Fe(II) dissolution increases with increased bacteria concentration as more organic acid are produced which led to an increase in both the brightness and whiteness of the kaolin (Zegeye, et al., 2013). However, higher pulp density produces a lower concentration of organic acids by bacteria. The Fe reduction rates increased with lower pulp density because the Fe reduction rate depends on the amount of organic acids produced by bacteria (Arslan and Bayat, 2009).

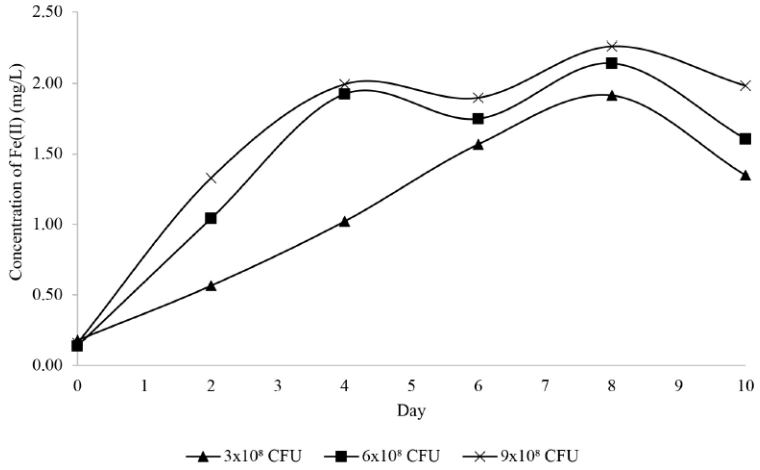

Figure 2.5: Dissolution of Fe at various bacteria concentration (Yap, et al., 2020).

It was also found in a study that during the first 15 days of bioleaching, the Fe dissolution rate of the samples was higher when kaolin was added on the third day (Hosseini, et al., 2007). This is because during the first 15 days, the microorganisms are going through the adaptation process. After that, the microorganisms that were adapted can perform better since the strains are adapted to the environment they are placed in after 15 days. The Gram-positive bacteria Fe reduction properties very much rely on the media composition. Iron-reducing capabilities of the microbes are impacted by different culturing conditions of the bacteria (Jing, et al., 2021). The removal of Fe impurities from the kaolin depend significantly on inoculation with the Fe(III) reducing bacteria and the initial population of the organisms with particular nutrients included in the culture medium (Guo, et al., 2010). As demonstrated by Lee, et al. (2002), the ferric iron reduction only becomes significant when inoculated with IRB.

2.6 Ways to Enhance the Bioleaching Process

There are various ways discovered throughout the years to enhance the extraction of Fe through bioleaching in order to increase the efficiency and improve the Fe extraction from kaolin. The Fe(III) reduction rates depends on microbe to clay ratio, surface area of clay minerals, pH of medium, aqueous medium chemistry, temperature and the presence of electron-shuttling compounds (Peng, et al, 2019).

Arslan and Bayat (2009) found that there is a positive influence on the degree of success in the bacterial leaching of kaolin by increasing the proportion of fine-grained fraction. But Hosseini, et al. (2007) found that the percentage of Fe removal was lower when the particle loading is higher. This is because the increased amount of clay will produce a highly viscous culture media. It was suggested that for organic bacteria to be effective, increased viscosity would change the clay particle aggregation and decrease the available surface area.

An increase of the pH value from 6 to 7.5 decreased removal of Fe impurities from kaolin and reached a minimum between pH 7.5 and 7.9 (Guo, et al., 2010). Study by He, Huang and Chen (2011) had a different result whereby the leaching of Fe(III) was enhanced at higher pH in the medium. Štyriaková, Štyriak and Malachovský (2007) also found that low pH during the incubation result in Fe(III) not reduced during abiotic reduction of Fe(III) because the uninoculated medium was acidified.

But in some research where glucose is added to the bacteria to monitor the activity of the bacteria, glucose concentration gradually decreased when the pH was maintained in the range of pH 6 – 7. The bacterial activity was reduced when pH values were lower than 6 and at pH values 5 and below, the consumption of glucose were eventually stopped and therefore indicating that the bacterial activity were stopped (Štyriaková, Štyriak, Nandakumar and Mattiasson, 2003). This is because the bacteria require optimum condition to cultivate, when the bacteria are under acidic condition, the bacterial activity becomes low and consumes less glucose. However, if sufficient time is given, bacteria might adapt to the acidic condition and continue to consume glucose. Since an increase in pH value reduce the removal of Fe and low pH inhibit the microbial activity, an optimum condition is required to maintain microbial activity and Fe removal rate.

The rate of Fe reduction and dissolution in the bioleaching process could be enhance by the presence of yeast extract, addition of nitrate and sulphate in the medium (Štyriaková, Štyriak and Malachovský, 2007). Increased sucrose concentration would also increase the removal of Fe impurities (Guo, et al., 2010). This is because glucose or sucrose has carbon as

an energy source for biological metabolism such as fermentation for heterotrophic bacteria (Štyriaková, et al., 2010).

The indigenous microorganisms could remove Fe(III) impurities but addition of bacteria *B. cereus, B. megaterium* strains and chelator Na_2EDTA greatly enhanced the process (Štyriaková, et al., 2010). The bioleaching rate was accelerated with addition of different nitrate such as $(NH_4)_2SO_4$ and the bioleaching medium added with $Co(NH_2)_2$ and $(NH_4)_2SO_4$ enhanced the sample Fe dissolution (Guo, Lin, Xu and Chen, 2010). In a study by He, Huang and Chen (2011), Fe dissolution was also enhanced by addition of chelator nitrilotriacetic acid (NTA). The addition of organic feedstock during bioleaching promoted the growth of inoculated *Bacillus* spp. and indigenous heterotrophic bacteria while the Na_2EDTA chelator contributed to the higher Fe dissolution in anaerobic condition, *Bacillus* strains clearly produced the highest yield of Fe reduction and dissolution in the experiment with the presence of chelators (Štyriaková, et al., 2010). This is in agreement with a study made by Blodau and Gatzek (2006), chelators such as NTA influence Fe(III) to be more readily available to microorganisms. Furthermore, oxalic acid could be utilized as electron donors and carbon source for microorganisms because Fe leaching from kaolin was enhanced by the oxalic acid added to the leaching solution. It was also found that addition of metals such as Fe(II) and Mn(II) ameliorated the dissolution of Fe (He, Huang and Chen, 2011). The dissolution rate of Fe varied with different *Bacillus* spp. and increased upon the addition of 9,10-anthraquinone-2,6-disulphonic acid (AQDS) (Štyriaková, et al., 2007). Adding the known AQDS electron shuttle led to an initial higher reduction rate of Fe(III) than the rate of reduction without AQDS but has a similar extent of Fe(II) formation (Kappler, et al., 2014), indicating that the dissolution of Fe does not have a big difference after the addition of AQDS.

A study noticed that soil biogeochemistry could be influenced by biochar addition to soils, not only biogeochemistry but potentially soil physicochemical properties by directly mediating the processes of electron transfer (Kappler, et al., 2014). Addition of biochar at low concentrations has lower rates and extents of reduction than those with AQDS, it is even lower than those reductions without an electron shuttle, indicating that low biochar

concentrations has an inhibiting effect on microbial mineral reduction of Fe(III). But addition of higher concentrations of redox-active biochar particles at 5 gL^{-1} and 10 gL^{-1} stimulated electron transfer and it indicates that electron transfer can be stimulated by biochar itself functioning as an electron acceptor and transfer electrons to the Fe(III) mineral ferrihydrite through microbially reduced biochar. In an electron micrographs study of the rough surface of biochar particles by Kappler, et al., (2014), the cells and biochar particles distance including biochar and ferrihydrite particles distance are mostly larger than the 20 Å maximal distance essential for direct electron transfer. This justify why the presence of a combination of AQDS and biochar has the highest ferric reduction rate, because the gaps between biochar and cells or between biochar and ferrihydrite are bridged by AQDS (Kappler, et al., 2014).

Besides addition of chelators, carbon source and metals, pulp density is also one of the variable studied to enhance the bioleaching of iron. It was found that the lower amount pulp density, and clay added in the beginning of cultivation, achieve the highest Fe removal percentage (Hosseini, et al., 2007). The bacterial leaching activity increase as glucose concentration decreased continuously during the bioleaching time when the bacteria concentration is increased incrementally from 3×10^8 cfu to 9×10^9 cfu. The amount of Fe(II) in the solution also increased progressively, indicating the extraction of Fe corresponds with increase in bacteria count (Yap, et al., 2020).

According to Hosseini, et al. (2007), the most significant factor to affect the Fe leaching response is strain type. Different strains of bacteria may have different efficiency in leaching Fe from kaolin (Yap, et al., 2020), UKMTAR-4 strain of *B. cereus* had a higher percentage of Fe removal (53.9 %) as compared to *B. cereus* procured externally (33.9%). Jing, et al. (2021) illustrated that *B. cereus* is the most efficient bacteria in reducing Fe impurities and ferric(III) oxide in kaolin, followed by *S. aureus* which only remove Fe contaminants of kaolin. Štyriaková, et al. (2012) also found that the dissolution of Fe was higher when *Bacillus* species is present in the medium compared to indigenous heterotrophic bacteria. There was a 36.7% difference in amount of Fe removed after 31 days of bioleaching between indigeneous bacteria and inoculated *Bacillus* samples, but it decreased to 3.3% after 63 days of bioleaching (Štyriaková, et al., 2012). Although in long period of

bioleaching the difference is much smaller, industrial bioleaching normally does not take 2 months to remove impurities so the inoculated *Bacillus* will have great impact to the bioleaching method.

2.7 Microbial Fe Reduction of Impurities in Kaolin

Bioleaching utilise the acids secreted by fungi or IRB to leach Fe from kaolin with the original composition of kaolin conserved. Bacteria secrete organic acids and dissolution of Fe impurities from clay minerals is a result of organic acids production by bacterial metabolisms. The Fe on minerals was solubilized by organic acids secreted by *Bacillus* spp. thus reducing impurities in clay minerals (Yong, et al., 2022). Bacteria are able to extract Fe from different clay as Fe(III) may become the terminal electron acceptor for IRB but the local octahedral sheet Fe conditions determines the reversibility and magnitude of the reaction (Finck, Schlegel and Bauer, 2015). The dissolution of iron oxides known as redox reactions is the reductive mechanisms by organic acids. The organic acids undergo oxidation and electrons are released then iron oxides accept electrons through reduction to form soluble Fe(II) (Lee, et al., 2006). A reducing environment was expected as a result of the bacterial metabolic activities which could generate organic acids (Sanchez-Palencia, et al., 2022).

In either a growth or non-growth medium, electron acceptor is usually the structural Fe (III) in clay minerals while the electron donor is organic matter (Yong, et al., 2022).

2.8 Microbial Reduction Mechanisms in Clay Minerals

Two mechanisms are identified in microbial reduction of Fe in clay minerals, the solid-state reduction and dissolution-precipitation. Bonding and/or the symmetry properties change of octahedral and tetrahedral sheets are involved in solid state reduction mechanism while clay minerals dissolution and successive formation of biogenic minerals are observed in dissolution-precipitation mechanism.

2.8.1 Solid State Reduction

Microbial reduction of Fe(III) occurring in solid state reduction mechanism has no dissolution of minerals as biogenic minerals were not formed (Seabaugh, et al., 2006). In the solid state reduction mechanism, Fe-bearing smectites crystal structures are modified in terms of symmetry properties and/or bonding, but reoxidation can fully reverse the changes (Yong, et al., 2022).

2.8.2 Dissolution-precipitation

In dissolution-precipitation microbial reduction mechanism, a certain degree of dissolution was implied from the biogenic products formation, release of a substantial fraction of Fe(III) as well as changes in cation exchange capacity (CEC) and specific area changes during reduction and reoxidation (Yong, et al., 2022).

During Fe(III) reduction, CEC of minerals was increased and it will not restore to the initial CEC upon reoxidation due to permanent K^+ fixation and the secondary phase minerals formation within the mineral structure (Koo, et al., 2014).

2.9 Inconsistency of Iron (Fe) Reduction Mechanism

The inconsistency of Fe reduction mechanism may be due to the type of medium that affect the Fe reduction mechanisms such as the presence of different carbon sources, for example glucose in growth medium promotes better efficiency of removal of Fe from kaolin for Fe(III)-reducing bacteria (Guo, et al., 2010). There are a few possibilities for bacteria to adhere to minerals surface, which includes hydrophobic and electrostatic interactions as well as biofilms formation, which is a result of bacterial cells aggregation on minerals surface. Cation-bridges between clay and bacteria may form through the released cations such as Na(I) and Ca(II) while adhesion of cells to clay minerals are assisted by the chelating effect of extracellular polymeric substances (EPS).

2.10 Primary Adhesion of Bacteria

The reversible bacterial adhesion in the first stage will be determined by hydrophobic and electrostatic interactions. Clay particles surfaces are negatively charged and will bind onto cations and attach on surface of minerals. Next, on mineral surface the negatively charged ions are attracted by the remaining positive charges on cations to form double diffuse layers. The electro-repulsive forces between minerals and bacterial cells suppressed cell adhesion in EPS-poor strain because of the electrical double layers. But the polymeric interaction will enhance cell adhesion when there is a large amount of EPS (Yong, et al., 2022). A study proposed that the decisive factor for cell adhesion is electrical force as the polymeric interaction is weak and van der Waals force depends on distance (Tsuneda, et al., 2003).

The electrostatic repulsive forces effect between mineral surface and bacterial cell decreases due to the hydrophobic character of bacterial cell. A less hydrophobic character is exhibited from cell surfaces that are having more charges. Therefore, higher hydrophobicity bacterial cells are easier to adhere to mineral surface (Natarajan, 2018). Furthermore, the hydrophobicity and electrostatic attraction decreases at high pH of the solution which leads to hindrance of bacteria adhesion onto mineral surface.

2.11 Second Stage Adhesion of Bacteria

Second stage of interaction between microbe and mineral is an irreversible process and occurs through EPS secretion (Yong, et al., 2022). Bacteria produce EPS to fill the intercellular space of microbial aggregates which bring about the biofilm formation (Vu, et al., 2009). Other than entanglement of EPS which contributes to the stability of matrix, hydrogen bonds, electrostatic interactions as well as van der Waals interactions between EPS components are the types of binding forces that affects the stability of biofilm matrices.

2.12 Summary

Generally, bioleaching is considered as a preferred alternative over the conventional way of extracting Fe through chemical leaching and magnetic separation. Each studies had different amount of leached Fe from kaolin and the amount of leached and solubilized Fe is dependent on the geochemical

transformation processes of rocks, not proportional to the initial Fe content of kaolin samples. This is because each sample of kaolin has slightly different mineralogical composition and distribution of Fe minerals in silicate matrix (Štyriaková, Štyriak, Malachovský and Lovás, 2006). The efficiency of Fe extraction and dissolution is also dependent on different condition the samples are placed in, geographical source and methods of kaolin processing affects their specific physical and chemical properties (Hernández, et al., 2013). The different mechanism of microbial reduction and its inconsistency was also discussed.

From the literature review of previous studies, it can be concluded that Bacteria of *Bacillus* spp., *Aspergillus* spp. and *Shewanella* spp. can reduce the content of free Fe as well as of Fe bound in mica that contaminates kaolin. Bioleaching does not only extract Fe but the kaolin samples are also enriched by fine-grained fraction and transitioned from a more amorphous form to crystalline form without affecting the mineralogy. This process is more time consuming from technological view and requires optimisation but is more advantageous in ecology and economical cost aspects (Štyriaková and Štyriak, 2000).

CHAPTER 3

METHODOLOGY AND WORK PLAN

3.1 Introduction

The overall methodology of the project can be separated into several sections as summarized in Figure 3.1 which includes preparation of reagents and sub-culture, nutrient optimisation, bioleaching experiment and analysis of the results. Gantt chart in Picture B-26 and Picture B-27 of appendix shows the overall project planning.

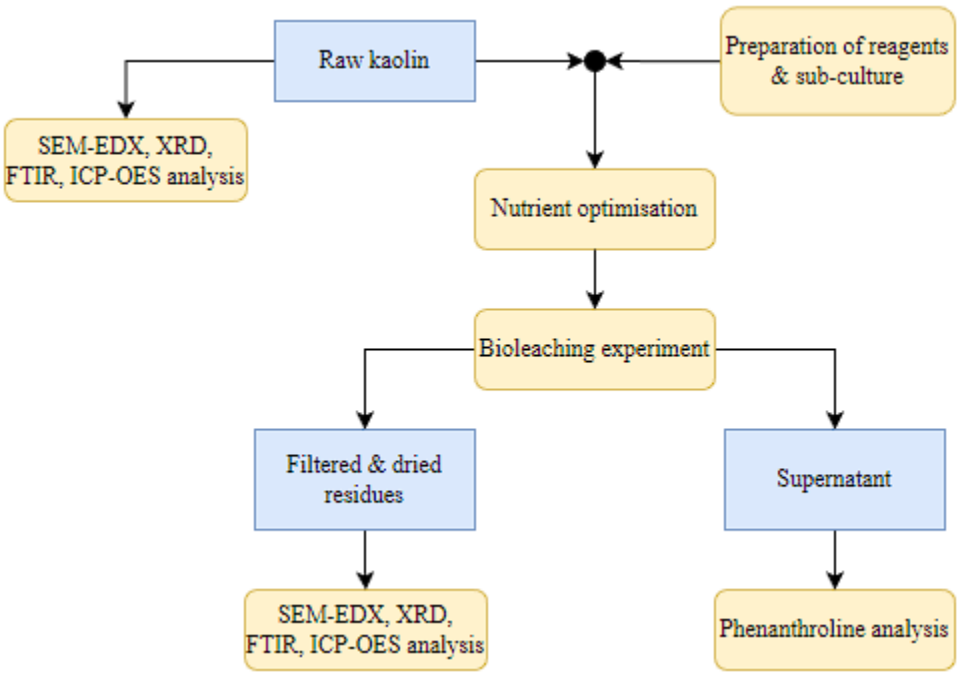

Figure 3.1: Overall methodology.

The experiment was carried out in the two stages method whereby the bacteria cultures were prepared and placed into the conical flask after incubation to bioleach both the Malaysian and Chinese kaolin. Next, the supernatant of the bioleached kaolin was analysed with photospectrometer through the phenanthroline analysis for day 0, 5 and 10. Then, the bioleached kaolin was filtered with 11 µm filter paper and the residues were dried in drying oven at 80 °C for approximately 24 hours to be analysed under SEM-EDX, X-ray Diffraction, FTIR and ICP-OES analysis for day 0 and day 10.

The methodology of the experiment was referenced from the spectrophotometric method for the ferrous iron determination in the presence of ferric iron by Herrera, et al., 1988; Muir and Andersen, 1977 and other prior methodologies done by other researches.

3.2 Chemical and Materials

There are various materials and chemical required for the bioleaching experiment. Table 3.1 shows the list of materials and chemicals that were used in the experiment with the estimated quantity and their usage. The chemicals and equipment for analysis are shown in Appendix B.

Table 3.1 List of Materials and Chemicals.

Material / chemical	Estimated quantity	Usage
Malaysian kaolin	100 g	Clay sample.
Chinese kaolin	100 g	Clay sample.
Aluminium foil	-	Cover samples for autoclave, avoid contamination of samples.
1,10 – Phenanthroline monohydrate	0.8 g	O-phen solution.
Distilled water	-	Preparation of reagents.
Hydrochloric acid	200 µL	To dissolve phen powder.
Lb broth	10 g	LB broth solution.
Ammonium acetate	12.33 g	Stabilize pH for phenanthroline assay.
Glacial acetic acid	30 mL	To dissolve ammonium acetate.
Ammonium iron (II) sulphate hexahydrate	0.1755 g	Preparation of standard solution for ICP analysis.
Concentrated sulphuric acid	93 mL	Preparation of standard solution for ICP analysis, acid digestion and Preparation of NaF.

Nitric acid	270 mL	Dilution of standard solution.
Glucose	35 g	Carbon source.
Sodium fluoride	0.168 g	Make sure phenanthroline assay identify Fe(II) ions.
Deionized water	300 mL	Dilution of digested kaolin.
Filter papers	20 pieces	Filtration for samples and filtration sterilization of glucose.

3.3 Preparation of Kaolin Sample

10 g of Malaysian kaolin was measured and filled into a 500 mL conical flask using spatula and weighing boat. The conical flask was then covered with aluminium foil and autoclaved. After autoclave, the kaolins were left to dry in drying oven at 60 °C. The same steps were repeated for Chinese kaolin. 4 sets for each types of kaolin were prepared for three types of bacteria and an abiotic control.

3.4 Preparation of Reagents

The reagents that were prepared includes phenanthroline assay, sub-culture, nutrients, carbon source for the bacteria to grow and other reagents that improves the results of the experiment.

3.4.1 O-phen Solution (0.8 %) preparation

The O-phen solution is the colorimetric solution to show the presence of Fe(II) in the medium. First, 30ml of distilled water was measured and poured into a 100 mL beaker, then 0.8 g of 1,10-Phenanthroline monohydrate powder was weighed and added to the distilled water followed by 200 µL of hydrochloric acid (HCl) using pipette. After all the 1,10-Phenanthroline monohydrate powder had dissolved, distilled water was added up to total volume of 100 mL. Next, stirrer was placed into the beaker and the mixture was stirred at 60 °C. Throughout the process, the o-phen solution was covered with aluminium foil to avoid exposure to light as it is light sensitive.

3.4.2 Lysogeny Broth (Luria-Bertani Broth) preparation

The LB broth was prepared in a 500 mL glass bottle. Firstly, 10 g of LB broth was weighed and added into the glass bottle. Then, distilled water was added up to 500 mL.

3.4.3 Ammonium acetate preparation

The ammonium acetate solution was prepared by first producing the master stock. Then, the working stock was prepared from the master stock. The master stock was prepared in a concentration of 3.2 M in a 50 mL falcon tube while the working stock was prepared in a 100 mL glass bottle with a concentration of 1.28 M.

Number of moles for 3.2 M of ammonium acetate ($NH_4CH_3CO_2$) was computed with Equation 3.1, then the required mass of ammonium acetate powder was calculated using Equation 3.2 as shown below. The required volume of master stock to prepare 100 mL of 1.28 M ammonium acetate was calculated using the dilution equation as shown in Equation 3.3.

$$n = MV \tag{3.1}$$

where

n = mole

M = molarity, mol/L

V = volume, L

$$n = \frac{m}{M'} \tag{3.2}$$

where

n = mole

m = mass, g

M’ = molar mass, g/mole

$$M_1V_1 = M_2V_2 \quad (3.3)$$

where

M_1 = Concentration of stock solution, mol/L

V_1 = Volume of stock solution, mL

M_2 = Concentration of diluted solution, mol/L

V_2 = Volume of diluted solution, mL

Firstly, the 50 mL falcon tube was filled with 10 mL of distilled water. Next, 12.33 g of ammonium acetate powder was weighed and added into the falcon tube followed by 30 mL of glacial acetic acid for the ammonium acetate powder to dissolve. After it is dissolved, 10 mL of distilled water was added to top up to a total volume of 50 mL ammonium acetate solution.

After the solution is thoroughly mixed, the working stock was prepared by adding 40 mL of master stock into a 100 mL glass bottle. Next, distilled water was topped up until the glass bottle has volume of 100 mL.

3.4.4 Glucose solution (10 g/L) preparation

The glucose solution was prepared by filling up some water in a 1 L glass bottle. Then, 10 g of glucose powder was weighed and added into the distilled water. After the powder had dissolved, distilled water was topped up to total volume of 1 L.

In order to make sure there is no bacteria within the glucose, a 0.22 nm filter paper and vacuum pump was used to carry out filtration sterilization on the glucose solution as shown in appendix Picture B-12.

3.4.5 Sodium fluoride (NaF) solution (0.4 M) preparation

Sodium fluoride, NaF solution was prepared and added into the phenanthroline assay to ensure the phenanthroline assay identify Fe^{2+}, giving a more reliable results in phenanthroline analysis. Equation 3.1 was used to compute number of moles for 0.4 M of NaF, and Equation 3.2 was used to compute the mass of NaF powder required.

The 0.4 M NaF was prepared by filling a 15 mL falcon tube with 5 mL of distilled water. Then 0.168 g of NaF powder was added to dissolve in the distilled water. After the NaF powder dissolve, 200 µL of sulphuric acid (H_2SO_4) was added and the falcon tube was filled with distilled water until it reached total volume of 10 mL. The NaF solution was prepared each day for day 0, 5 and 10 to ensure each analysis uses a freshly prepared NaF.

3.4.6 Sub-culture preparation

Sub-culture was prepared to ensure that the bacteria is active for the bioleaching process. First of all, 10 mL of the previously prepared LB broth was measured and poured into a 50 mL falcon tube. Then, a scope of single colony bacteria that was stored in glycerol stock at -80 °C was taken and added into the falcon tube using sterilised pipette tip. The mixture was vortexed and incubated at 250 rpm and 37 °C for 16 to 18 hours. The steps were repeated for all the three types of bacteria.

3.5 Nutrients Optimisation

The optimum nutrients required for the bioleaching process was determined by using different concentration of glucose and comparing the results after 5 days of bioleaching. The different nutrient condition for the bioleaching process by previous studies are list in Table 3.2 below.

Table 3.2: Various nutrient condition for microbial reduction of kaolin.

Štyriaková and Štyriak, 2000	100 ml of modified Bromfield medium (KH_2PO_4 0.5 g/l, $MgSO_4.7H_2O$ 0.5 g/l, $(NH_4)_2$ SO_4 1.0 g/l, NaCl 0.2 g/l, glucose 20 g/l), anaerobic condition.
Guo, et al., 2010	100 mL of 10 g/L glucose medium, 5 mL of mixed culture broth.
Zegeye, et al., 2013	10mM of HCOONa and kaolin (10 g to 20 g) as electron donor and final electron acceptor, 0.9% of NaCl and 100 µM of AQDS. Incubate 20 to 30 °C in the dark, rotate 320 rpm.
Yap, et al., 2020	80 mL of glucose solution, kaolin (10 g), 30 °C, rotate at 250 rpm.

In this experiment, the different nutrient concentration used were 60 g/L, 80 g/L and 100 g/L of glucose, incubated at 30 °C 250 rpm. The optimum glucose concentration that was determined from the nutrient optimisation experiment was then used to conduct the bioleaching of both Malaysian and Chinese kaolin.

3.6 Bioleaching of kaolin

The bioleaching process took place for 10 days. The sub-cultures were diluted first by a ratio of 1:3, 2 mL of LB broth was mixed with 1 mL of bacteria culture in micro-centrifuge tubes using pipette. The sub-culture was replaced with distilled water for 'blank' sample. The dilution was performed using the aseptic technique to avoid any contamination and the diluted mixture was vortexed to ensure it is fully mixed. Next, two cuvettes were prepared with one filled with 'blank' and the another cuvette filled with the diluted bacteria culture. To find the volume of bacteria sub-culture to be added for bioleaching, the cuvettes was placed in the cell density meter (Ultrospec 10) to determine the optical density (OD) value, the optical density value was taken from the average of three readings for better accuracy. Then the actual OD value was calculated with the Equation 3.4 below.

$$A = Y \times 3 \tag{3.4}$$

where

A = actual OD value

Y = average OD value of the cell density meter

The amount of each bacterium from the sub-culture required to be added to the kaolin samples was calculated by Equation 3.5 below. And the volume of bacteria to be added into kaolin was determined from Equation 3.6.

$$\mathrm{c} = A \times (5 \times 10^8 \, \frac{cfu}{mL}) \tag{3.5}$$

where

c = actual concentration of bacteria, cfu/mL

A = actual OD value

$$V = \frac{9 \times 10^8 \, cfu}{\mathrm{c}} \tag{3.6}$$

where

V = volume of bacteria to be added to kaolin, mL

c = actual concentration of bacteria, cfu/mL

The kaolin samples in the conical flask was first added with 100 mL glucose. Next, the volume of bacteria culture as determined from the above Equation 3.6 was added into the kaolin. Lastly, the kaolin was placed into the incubator for incubation at 30 °C and 250 rpm for bioleaching.

3.7 Centrifugation

Centrifugation of the sample was done to obtain the supernatant for phenanthroline analysis. Firstly, 1 mL of the sample was pipetted into a micro centrifuge tube. Next, the micro centrifuge tube was placed into centrifuge (Eppendorf) to separate the suspension into supernatant and precipitate. The conical flask containing the sample was placed back into incubation at 30 °C and 250 rpm. There was a total of 8 centrifuge tubes which includes the three bacteria-clay sample for both Malaysian kaolin and Chinese kaolin, one abiotic control sample for both Malaysian kaolin and Chinese kaolin.

3.8 Phenanthroline assay

Phenanthroline assay was carried out to analyse the Fe(II) concentration in the supernatant. A new set of micro centrifuge tubes was prepared and 500 µL of NaF was added followed by 200 µL of o-phen solution. Similarly, 200 µL of ammonium acetate was added to the mixture to stabilize the pH. Lastly, 100 µL of the sample supernatant was added, distilled water was used to replace the supernatant for ‘blank’ sample. The mixture was vortexed after each addition of new reagents for even mixture. All the micro centrifuge tubes

containing the supernatant and phenanthroline assay were incubated in dark for an hour.

After incubation, the phenanthroline assay was transferred into cuvettes to measure the absorbance value in Nanodrop 2000 spectrometer at 492 nm. A total of ten sets of results will be obtained for Malaysian kaolin and Chinese kaolin to calculate the average absorbance value. The concentration of Fe(II) in the phenanthroline assay was determined by the relationship between the Fe(II) concentration and absorbance values for different Fe(II) values. The standard curve relationship was developed by Yong (n.d.) using a Fe(II) salt with different concentration and measuring the absorbance value of each concentration. The developed relationship y = 0.01x was shown in appendix Graph A-1.

3.9 Scanning Electron Microscopy (SEM) analysis

The effect of iron removal was observed on the morphology change of kaolin by using SEM (Hitachi, S-3400N). The dried bioleached kaolin samples were coated with gold prior to the analysis. The morphology changes of kaolin before and after the experiment was analysed and discussed in the results and discussion section.

3.10 Energy Dispersive X-Ray Spectroscopy (EDX) analysis

EDX (Hitachi, S-3400N) is a microchemical analysis technique used in conjunction with SEM. The mineral composition of the kaolin such as O, K, Al and Fe was analysed before and after the experiment. In EDX analysis, bioleaching efficiency was calculated by the changes of Fe composition before and after bioleaching as shown in Equation 3.7.

$$Bioleaching\ efficiency\ (\%) = \left(\frac{X_i - X_f}{X_i}\right) \times 100\% \qquad (3.7)$$

where

X_i = weight percentage of Fe composition in kaolin before bioleaching, wt %

X_f = weight percentage of Fe composition in kaolin after bioleaching, wt %

3.11 X-ray diffraction (XRD) analysis

XRD (Shimadzu, XRD6000) is an analysis technique to determine the crystalline structure of the kaolin particles before and after bioleaching process. The kaolin sample was placed into sample holder and analysed by using X-ray diffractometer. The XRD pattern was collected over a range of 10° to 80° 2θ using Cu Kα radiation (40 kV, 40 mA), with a 0.05° step width and a nominal collecting time of 30 seconds per 1°. Then the XRD pattern of the treated kaolin samples was compared with the untreated samples to analyse the effect of bioleaching on the structural changes of kaolinite.

3.12 Fourier Transform Infrared Spectroscopy (FTIR) analysis

FTIR is a technique used to study the bond formation between the mineral surface and bacteria during bioleaching process. The dried treated sample was placed on the sample holder of FTIR (Nicolet, IS10) to record the infrared absorption spectra. Since the organic structure of bacteria composed mainly of polysaccharides and lipids (protein), this analysis was used to determine the adsorption of bacteria onto the Fe(III) on surface of mineral through the OH and/or the COOH of both of the polysaccharides or the bacteria's protein fractions. The formation of hydrogen bond, if any, will allow us to elucidate the attachment mechanism of the bacteria cell onto the kaolin particles. The analysis was repeated with both treated and untreated Malaysian and Chinese kaolin to observe the difference before and after bioleaching.

3.13 Acid digestion using microwave digester

The acid digestion using the microwave digester (Berghof 'Speedwave four') was carried out on all the dried treated and untreated kaolin samples before conducting Inductively Coupled Plasma Optical Emission Spectroscopy (ICP-OES). First, the digester vessels are filled with approximately 9 mL of concentrated nitric acid and placed into the microwave digester for pre-digestion cleaning set at 200 °C for 35 minutes. After pre-cleaning, the vessels are still in high temperature and pressure, thus are left to cool down before opening it in the fume hood and disposing the nitric acids into labelled chemical waste bottles. Next, for the digestion of the dried kaolin powder, 9 mL of concentrated sulphuric acid was carefully added into the vessels

followed by 100 mg of dried kaolin powder samples. The vessels are then placed into the microwave digester and tightened to prevent leakage. Then the digester was set to temperature of 240 °C, 35 bar pressure, ramp up time of 1 minute and duration of 45 minutes digestion with 60 % power for step 1, while for step 2 the digester was set to temperature of 50 °C, pressure of 25 bar, ramp up time of 1 minute and 10 minutes digestion duration at 0 % power. When the microwave digester stopped, the vessels were left to cool down for around 30 minutes. Post-cleaning was also done with the same procedure and settings of pre-cleaning after the acid digestion to make sure there is no leftover samples or acid in the vessels. Then, the digested kaolin was diluted in the ratio of 5 mL of digested kaolin solution to 145 mL of deionized water as the digested kaolin was mixed with concentrated sulphuric acid during the digestion which is not suitable for ICP analysis unless diluted.

Since V_1 is 5 mL of the digested kaolin solution of and V_2 is the total volume after deionized water was added for dilution, which is 200 mL, the dilution factor was calculated to be 40 using Equation 3.2.

Lastly, the diluted kaolin solution was filtered with filter paper and syringe filter with 0.45 µm membrane filter to make sure the samples for ICP was free from any micro-precipitate. All the procedures were done in fume hood for safety purposes.

3.14 Inductively Coupled Plasma Optical Emission Spectroscopy (ICP-OES) analysis

The ICP-OES analysis requires a standard solution to build the calibration curve to determine the amount of Fe in kaolin. Firstly, the standard solution was prepared in 100 ppm by adding 100 mL of deionised water to 0.1755 g of ammonium iron(II) sulphate hexahydrate. Then, add with 2.5 mL of sulphuric acid for ammonium iron(II) sulphate hexahydrate to dissolve and topped up with deionised water to 250 mL. Since 100 ppm = 100 µg/m/L, required volume of 100 ppm standard solution is 250 mL, molar mass of Fe is 55.845 g/mole and molar mass of ammonium iron(II) sulphate hexahydrate is 392.14 g/mole. The mass required for ammonium iron(II) sulphate hexahydrate powder for preparation of 100 ppm standard solution was calculated using Equation 3.2.

In this experiment, the standard solution was prepared in 50 mL centrifuge tubes at concentration of 0 ppm to 100 ppm in increments of 20 ppm through dilution of the 100 ppm 250 mL standard solution prepared, the required volume of deionised water for dilution to obtain 0 ppm, 20 ppm, 40 ppm, 60 ppm, 80 ppm and 100 ppm standard solution was calculated using the dilution equation which is Equation 3.3.

The wash time for the before and after each analysis is 120 seconds to ensure there is no leakage of the samples or standard solution that might affect the results. After assigning new method, position of the standard solution and samples, the plasma was turned on and analysis was started with the calibration curve generation as shown in Graph A-2 in the appendix followed by the sample analysis to analyse the composition of Fe elements in both Malaysian and Chinese kaolin by using ICP-OES with wavelength of 238.2 nm. The calibration curve obtained was shown in part 4.8 in Figure 4.26 under Chapter 4 Results and Discussions. After the analysis, the Fe concentration of raw and bioleached kaolin from the results were multiplied with the dilution factor calculated previously in section 3.13 to obtain the actual concentrations, and the results were compared. The standard solutions and sample solutions are disposed into labelled waste bottles after analysis was done.

3.15 Summary

In a nutshell, there are two main parts in this experiment work plan which are bioleaching of kaolin from the prepared reagents and nutrients, and analysis of kaolin before and after bioleaching. One of the objective of this experiment is to determine the optimum nutrient (glucose) condition of bioleaching by analysing the Fe reduction of the sample and structural changes of Malaysian and Chinese kaolin. The milestones achieved in the first part of this project includes literature research, understanding basic concepts, phenanthroline method analysis was learnt in laboratory and the procedures, chemical preparation required as well as steps and settings for the analysis were recorded for the experiment to be carried out in second part of the project.

Table 3.3 below describe the parameters that may be optimized to attain higher iron removal from kaolin.

Table 3.3: Optimization Parameters.

Parameters	**Method**
Cell concentration/bacteria count	Change cell concentration added to the kaolin samples
Pulp density	Increase w/v %
Cell adaptation	Adding bacteria at different day but start day (Day 0) remains the same
Clay surface area	Use different proportion of fine-grained fractions
pH values	Change pH using acid/alkali and monitor using pH meter
Presence of yeast extract, addition of nitrate and sulphate	Add $(NH_4)_2SO_4$ and $Co(NH_2)_2$
Addition of chelators	Addition of Na_2EDTA or nitrilotriacetic acid (NTA)
Addition of metals	Addition of Mn(II) or Fe(II), may cause inaccurate measurement due to addition of iron
Addition of AQDS	Additrion of AQDS at predetermined concentration into bioleaching medium
Addition of biochar	Low concentration may have inhibiting effect
Types of strain	Use different types of bacterial strains (Already implemented with use of B. cereus, B. megaterium and B. aryabhattai)
Temperature	Different temperatures may yield different results for bioleaching

In FYP Part 2, the feasibility and practicality to study effects of each parameter was assessed based on availability of laboratory equipment and duration required. It was concluded that the selected parameter to be used to optimize the bioleaching experiment was nutrient (glucose) concentration.

CHAPTER 4

RESULTS AND DISCUSSION

4.1 Introduction

The results of the analytical techniques employed to characterise kaolin such as the SEM-EDX, XRD, FTIR as well as ICP-OES are presented in this chapter. The results of these work were also compared with latest studies involving bioleaching of kaolin with *Bacillus* species and other bacteria. The main difference of Malaysian and Chinese kaolin is the mineral composition in the kaolin as Malaysian kaolin has potassium (K) and magnesium (Mg) content as compared to Chinese kaolin. This difference in composition is also reflected on the XRD results. The Chinese kaolin also has a different structure, it is more elongated and narrow as compared to the Malaysian kaolin. The comparison between the kaolin from different origins, namely Malaysian kaolin and Chinese kaolin is further discussed in terms of surface morphology, structural changes, mineral composition and crystallography.

4.2 Nutrient optimisation

The nutrient optimisation experiment was conducted using the same methodology as the bioleaching experiment and the Fe reduction was measured using the phenanthroline analysis method with varying glucose concentration. This was conducted in order to determine the optimum glucose concentration for the actual bioleaching experiment. Due to time restrictions, only Malaysian kaolin was used as the basis of the optimum nutrient concentration for bioleaching. From the results shown in Figure 4.1, the optimum glucose concentration for bioleaching with *B. cereus* at day 5 was 6 g/L with the highest concentration of Fe(II) in the supernatant. While on the other hand, Figure 4.2 and Figure 4.3 depicted the optimum glucose concentration for bioleaching with both *B. megaterium* and *B. aryabhattai* was 10 g/L.

Due the optimum glucose concentration found in the nutrient optimisation experiment with kaolin bioleached with *B. cereus* had a different result compared to the two other species, the experiment was carried on for 10

days for further observations. On day 10, the optimum glucose concentration for bioleaching with *B. cereus* was found to be 8 g/L with a small difference of Fe(II) concentration between glucose concentration of 6 g/L and 8 g/L. Since the difference between using 6 g/L and 8 g/L glucose concentration was marginal, having a longer duration of 10 days bioleaching with glucose concentration of 8 g/L in the application of bioleaching may be less practical and costlier, should the process be scaled-up for industry. Hence, in the actual bioleaching experiment, the 6 g/L glucose concentration was used.

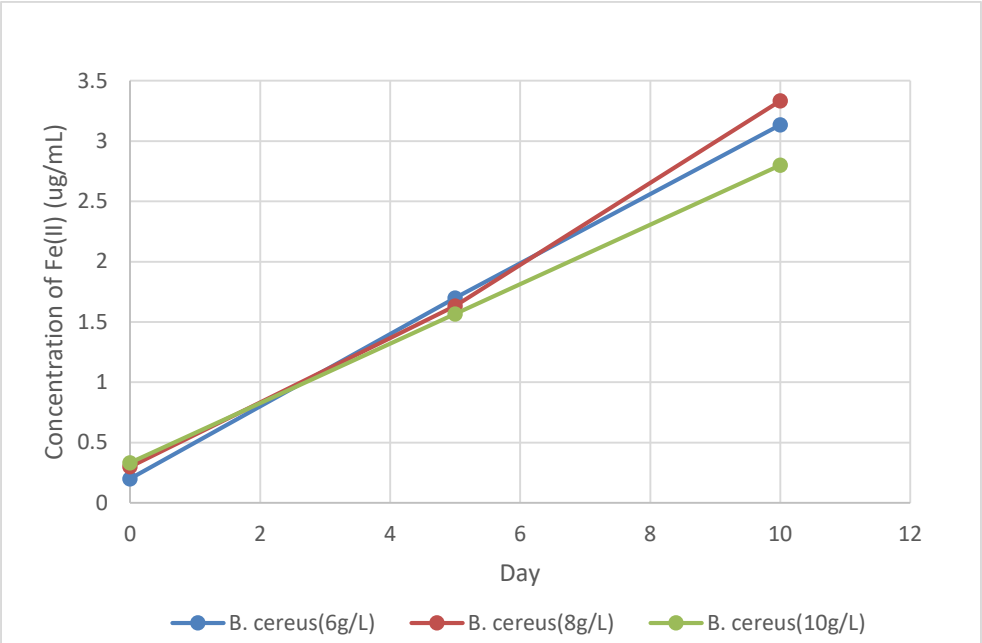

Figure 4.1: Fe(II) concentration of Malaysian kaolin bioleaching with *B. cereus* at different glucose concentration.

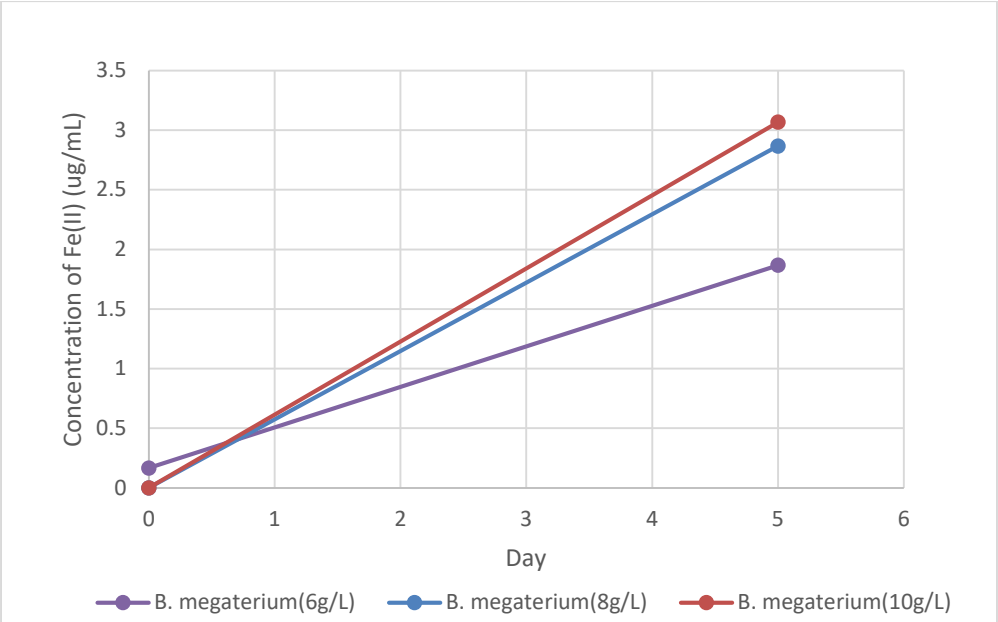

Figure 4.2: Fe(II) concentration of Malaysian kaolin bioleaching with *B. megaterium* at different glucose concentration.

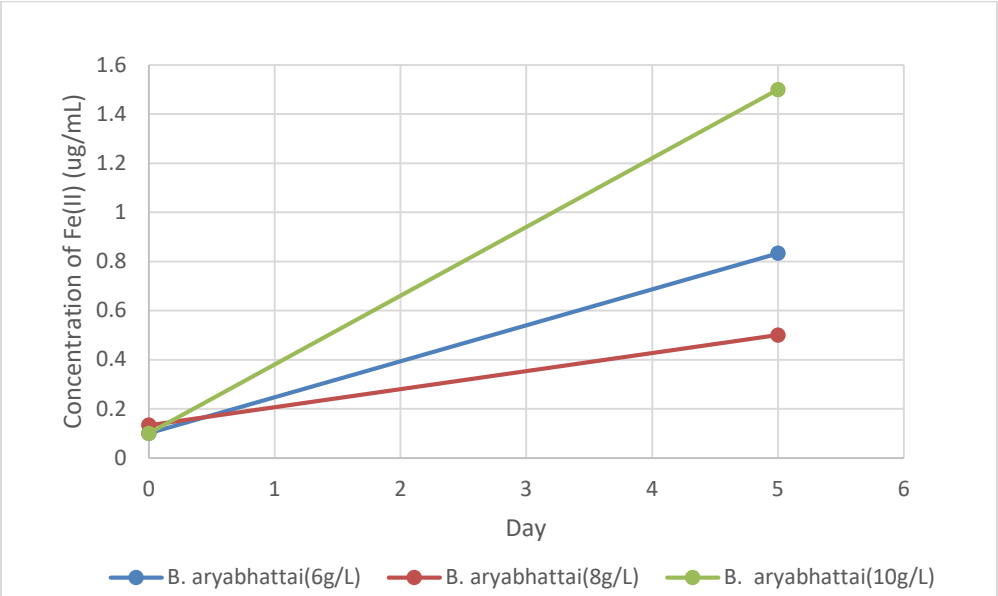

Figure 4.3: Fe(II) concentration of Malaysian kaolin bioleaching with *B. aryabhattai* at different glucose concentration.

4.3 SEM analysis of Malaysian and Chinese kaolin

The following SEM images shows the morphology and structures of both Malaysian and Chinese kaolin before and after bioleaching. Based on the SEM image at magnification of 4000 in Figure 4.4, the Malaysian raw kaolin has a more amorphous structure which could be seen circled in red whereby the

edges are much rounder and less sharp before bioleaching. The SEM image of abiotic control sample shown in Figure 4.5 has similar traits of a more amorphous structure with rounder edges. However, the SEM images of Malaysian kaolin bioleached with *B. cereus*, *B. megaterium* and *B. aryabhattai* are displayed in Figure 4.6, Figure 4.7 and Figure 4.8 respectively exhibit sharper edges and appears to be chipped or damaged in their structures as circles in red. This suggests that the Malaysian kaolin that were treated with the *Bacillus* bacteria had a more crystalline structure after bioleaching. In a previous study, SEM images also revealed a transformation of the kaolin surface from a more amorphous structure before bioleaching with bacteria, to a more crystalline structure after bioleaching (Yap, et al, 2020).

In the same way, it could be noted that in Figure 4.9 the Chinese kaolin had a more amorphous structure with rounder edges before bioleaching in the SEM image at magnification of 4000. In contrast, the SEM image of Chinese kaolin bioleached with *B. cereus*, *B. megaterium* and *B. aryabhattai* shown in Figure 4.10, Figure 4.11 and Figure 4.12 with 3500, 4000 and 5000 magnifications respectively appear to have visibly sharper and chipped edges in addition to the finer particles formed as indicated in red circles. This reveals that the structure of Chinese kaolin changed from amorphous to a more crystalline structure. It was evident in a research that the surface of the kaolin structure transitioned from a more amorphous structure before bioleaching to a more crystalline structure along with formation of finer particles (Guo, Lin, Xu and Chen, 2010). The structure of Chinese kaolin has long and narrow shapes as indicated in Figure 4.9, Figure 4.10, Figure 4.11 and Figure 4.12 before and after bioleaching which makes the identification of the changes to the structure difficult to be identified as the sharp edges of the structure are less noticeable, this was also observed and described as nanorod-like kaolinites structure in a study by Li, et al. (2015) and irregular elongated tubular shapes by Senoussi, et al. (2016). However, the narrow structure of the Chinese kaolin could be plausibly being made thin (leached) by the acid produced by the *Bacillus* bacteria (Brindley and Comer, 1955) as there are more narrow shape structure after bioleaching as shown in Figure 4.11 below.

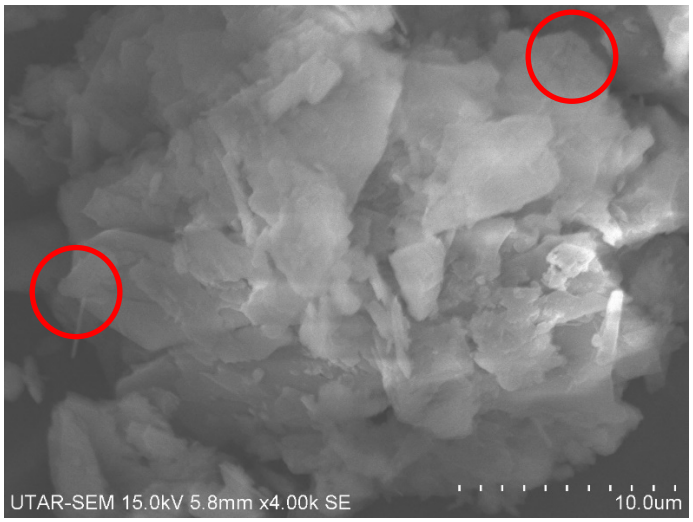

Figure 4.4: Untreated Malaysian raw kaolin.

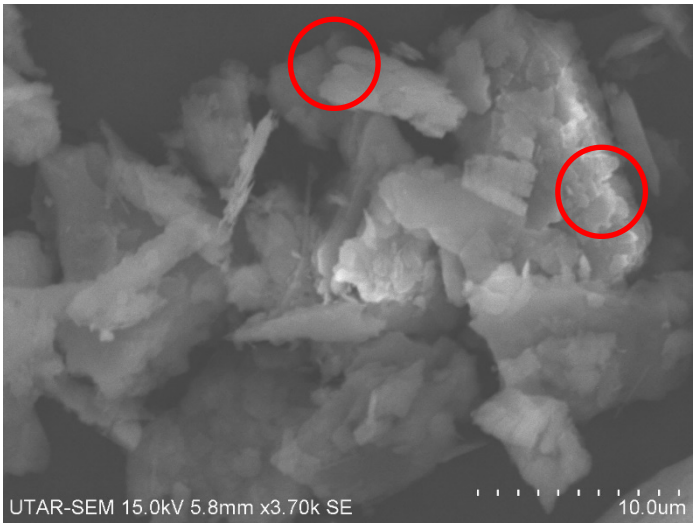

Figure 4.5: Malaysian kaolin without bacteria (control).

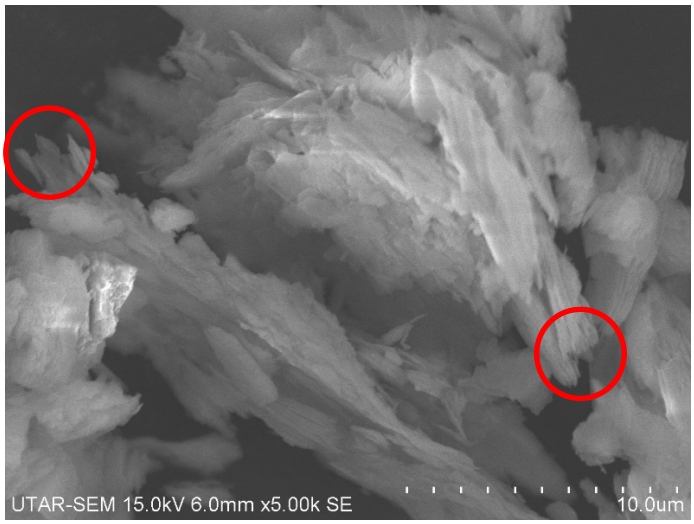

Figure 4.6: Malaysian kaolin treated with *B. cereus*.

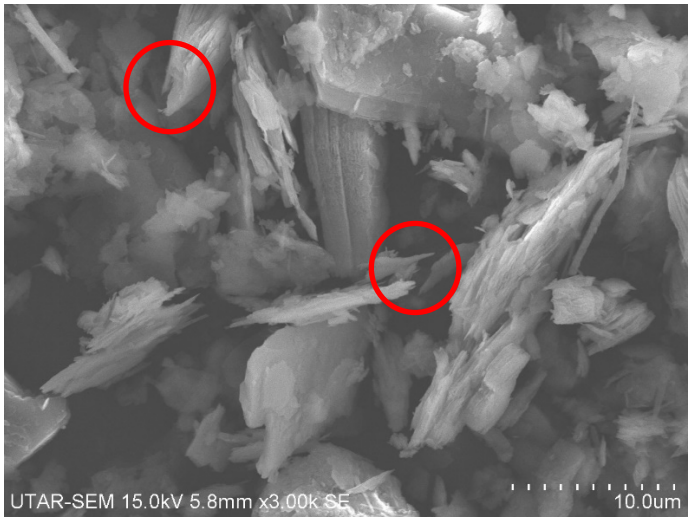

Figure 4.7: Malaysian kaolin treated with *B. megaterium*.

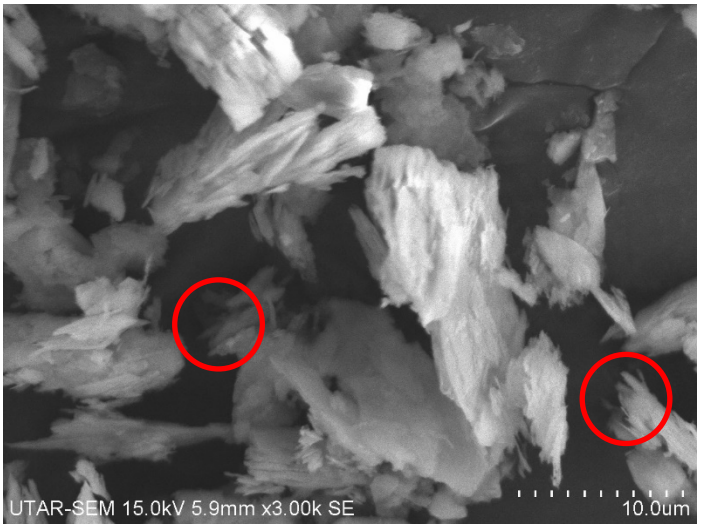

Figure 4.8: Malaysian kaolin treated with *B. aryabhattai*.

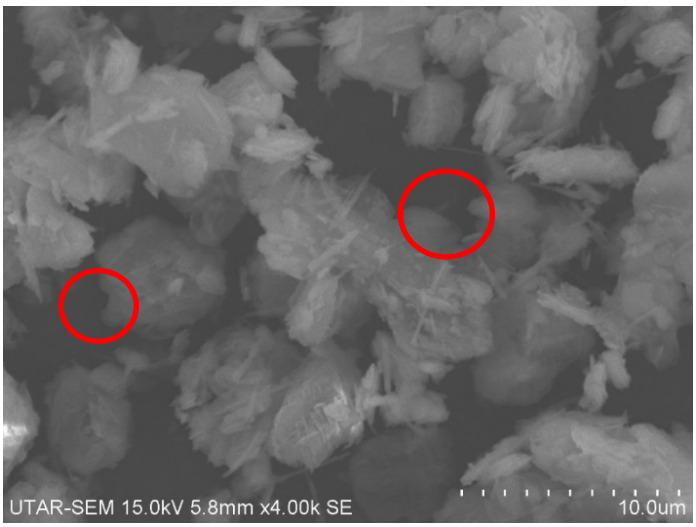

Figure 4.9: Untreated Chinese raw kaolin.

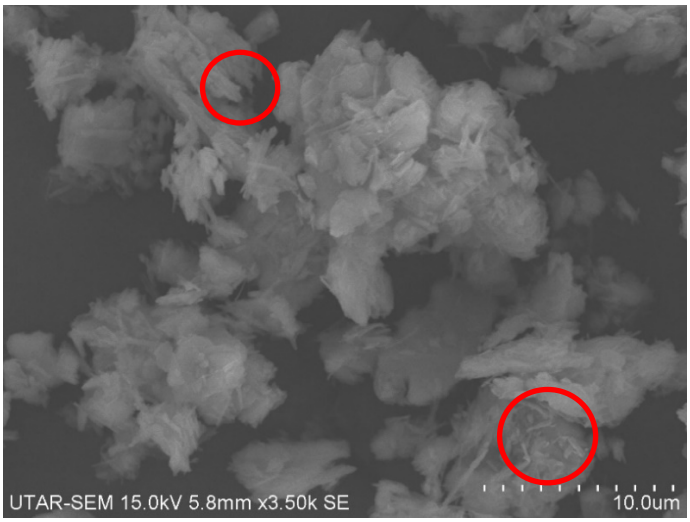

Figure 4.10: Chinese kaolin treated with *B. cereus*.

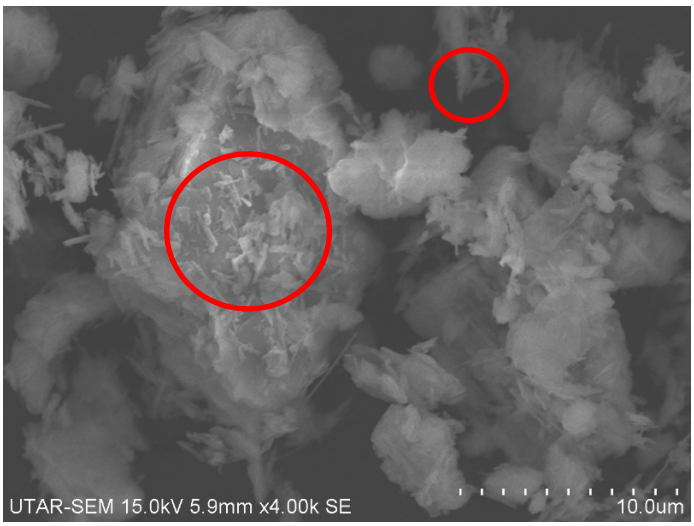

Figure 4.11: Chinese kaolin treated with *B. megaterium*.

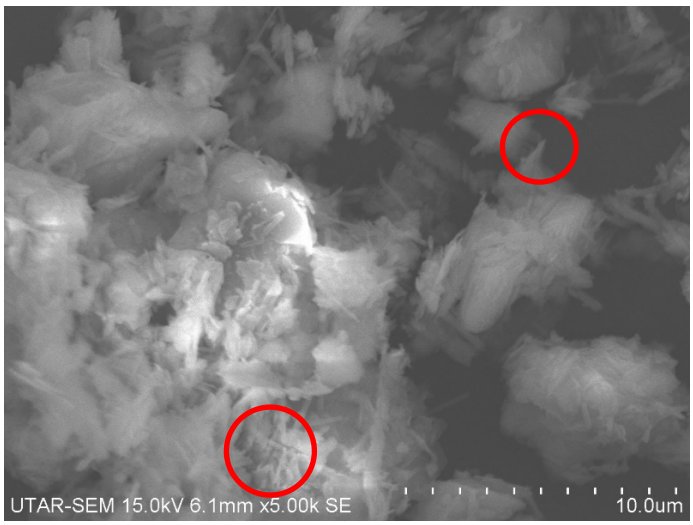

Figure 4.12: Chinese kaolin treated with *B. aryabhattai*.

4.4 Fe Reduction (Phenanthroline Analysis)

In bioleaching of both Malaysian and Chinese kaolin, insoluble Fe(III) in the kaolin is reduced to soluble Fe(II) (Zegeye, et al., 2013). This will lead to the supernatant of the bioleached kaolin having a higher Fe(II) concentration. Thus, the samples with higher Fe(II) concentration indicates a higher Fe(III) removal and efficiency in bioleaching. The concentration of Fe(II) was measured on day 0, 5 and 10 using the spectrometer as shown in Figure 4.13 and Figure 4.14.

Based on the results in Figure 4.13, the Malaysian kaolin has an overall increasing trend of Fe(III) reduction but the rate of Fe reduction reduced after day 5. The Fe(II) concentration of abiotic control surged from 0.30 µg/mL on day 0 to 1.47 µg/mL on day 5, then it increases slowly to 1.6 µg/mL on day 10. Additionally, Malaysian kaolin bioleached with *B. cereus* started with a Fe(II) concentration of 0.17 µg/mL on day 0 and then escalated to 1.57 µg/mL on day 5, it was then further increased to 2.63 µg/mL on day 10. For Malaysian kaolin bioleached with *B. megaterium*, the reduced Fe(II) concentration started with 0.07 µg/mL on day 0 and reached its peak at 2.10 µg/mL on day 5, however, it dropped to 1.83 µg/mL on day 10. And lastly, the Malaysian kaolin treated with *B. aryabhattai* increased from 0.03 µg/mL to 1.8 µg/mL on day 5 and then slightly increased to 2.13 µg/mL on day 10.

The Fe reduction in Chinese kaolin had a similar increasing trend as the Malaysian kaolin but with a higher concentration of Fe(II) on all day 0, day 5 and day 10 probably due to higher Fe dissolution as the structure of Chinese kaolin has smaller and narrower particle size as noted in the SEM images in section 4.5. It is evident that that the dissolution rate increases with decreasing particle size (Adekola, et al., 2017). It is also worth noting that kaolin that possess different surface morphologies varies in surface charge distribution (Li, etal., 2015) thus affecting the substitution of cations. As displayed on the graph in Figure 4.14, the Chinese kaolin abiotic control had a Fe(II) concentration of 1.6 µg/mL on day 0, and it increased to 2.9 µg/mL on day 5 before steadily increased to 3.47 µg/mL on day 10. Next, the Fe(II) concentration of Chinese kaolin treated with *B. cereus* rose from 1.67 µg/mL to 3.07 µg/mL from day 0 to day 10, it then remained almost constant up to

day 10 with a 3.17 µg/mL Fe(II) concentration. The Chinese kaolin bioleached with *B. megaterium* and *B. aryabhattai* also showed an increase of Fe(II) concentration from 1.57 µg/mL and 2.03 µg/mL respectively on day 0 to 3.6 µg/mL on day 5. Nevertheless, the Chinese kaolin bioleached with *B. megaterium* decreased slightly to 3.4 µg/mL while the Chinese kaolin bioleached with *B. aryabhattai* increased slightly to 3.8 µg/mL on day 10.

Generally, the bioleaching rate is highest from day 0 to day 10 for all the samples, the bioleaching rate will then slow down after day 5 showing barely any signs of bioleaching or even deteriorate. This result is in agreement with a study by Adekola, et al. (2017), whereby the rate of leaching was initially fast when kaolin is leached by acid, which in this experiment was referred to the acid produced by *Bacillus* species bacteria. However, the curves become almost flat in a very short period of time, after which the increase in the dissolution of Fe is almost negligible.

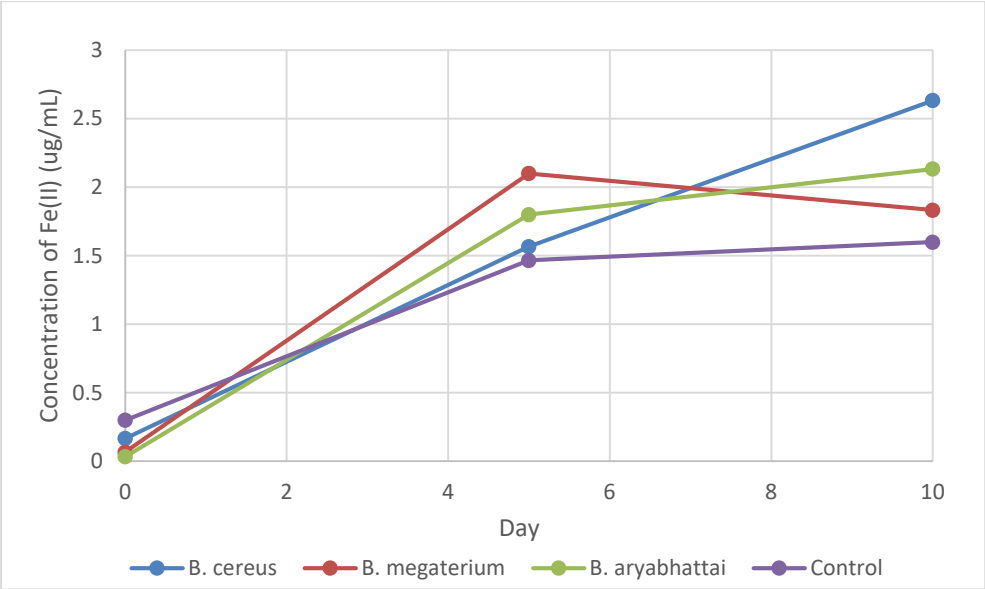

Figure 4.13: Graph of concentration of Fe(II) against day for Malaysian kaolin.

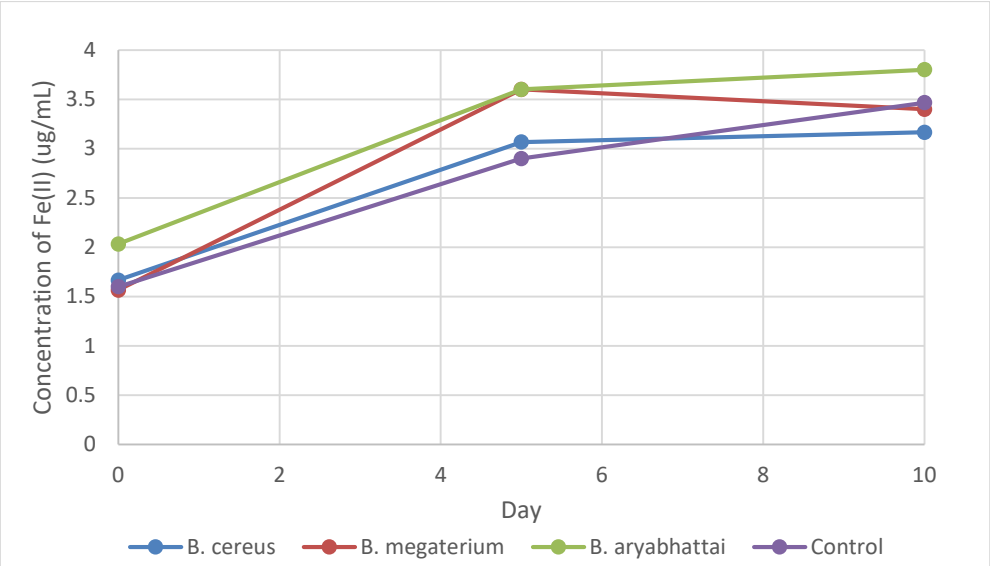

Figure 4.14: Graph of concentration of Fe(II) against day for Chinese kaolin.

4.5 Inductively Coupled Plasma Optical Emission Spectroscopy (ICP-OES) analysis

Inductively coupled plasma (ICP) analysis is used to identify the amount of Fe in the Malaysian and Chinese kaolin before and after bioleaching to verify that there is Fe reduction through bioleaching of kaolin. The effectiveness of the bioleaching of kaolin could also be shown through the ICP analysis. Firstly, from the calibration curve obtained through the standard solution shown in Graph A-2 in appendix, the linear regression has a coefficient of determination, R^2 of 0.999916 which provides that the results are reliable.

Next, based on the analysis results as shown in Table 4.1, Malaysian kaolin had a concentration of 40.84 mg/L of Fe before bioleaching which is very close to the amount of Fe in abiotic control of 37.88 mg/L. After bioleaching with *B. cereus*, *B. megaterium* and *B. aryabhattai*, the Fe concentration drops to 22.60 mg/L, 28.64 mg/L and 30.88 mg/L respectively. On top of that, Chinese kaolin had a Fe concentration of 35.04 mg/L before undergoing bioleaching. After bioleaching with *B. cereus*, *B. megaterium* and *B. aryabhattai*, the Fe concentration was reduced to 14.92 mg/L, 14.64 mg/L and 15.40 mg/L respectively.

Furthermore, the amount of Fe leached also known as the bioleaching efficiency was calculated using Equation 3.7, which is the bioleaching

efficiency equation from EDX analysis. The calculated values that are tabulated in Table 4.1 showed that the Fe removed from Malaysian kaolin bioleached with *B. cereus*, *B. megaterium* and *B. aryabhattai* are 44.7 %, 30.0 % and 24.4 % respectively. Besides, the amount of Fe leached for Chinese kaolin bioleached with *B. cereus*, *B. megaterium* and *B. aryabhattai* are 57.4 %, 58.2 % and 56.1 % respectively.

Table 4.1: ICP-OES results of Malaysian and Chinese kaolin.

		Diluted Fe(II) concentration (mg/L)	Actual Fe(II) concentration (mg/L)	Fe removed (%)
Malaysian kaolin	Raw	1.021	40.84	-
	Abiotic control	0.947	37.88	-
	B. cereus	0.565	22.60	44.7
	B. megaterium	0.716	28.64	30.0
	B. aryabhattai	0.772	30.88	24.4
Chinese kaolin	Raw	0.876	35.04	-
	Abiotic control	0.968	38.72	-
	B. cereus	0.373	14.92	57.4
	B. megaterium	0.366	14.64	58.2
	B. aryabhattai	0.385	15.40	56.1

4.6 EDX results and bioleaching efficiency

The EDX analysis identifies the composition of each element within the kaolin sample. Based on Table 4.2 and Table 4.3, the weight percentage of the elements has small change before and after bioleaching for Malaysian and Chinese kaolin except for Fe which shows an obvious decrease in weight percentage. It implies that there was Fe reduction from bioleaching without affecting the composition of the Malaysian and Chinese kaolin. The untreated Malaysian kaolin had 1.41 % of Fe before bioleaching and was dropped to 0.60 % for after treated with *B. cereus* while the weight percentage of Malaysian kaolin treated with *B. megaterium* and *B. aryabhattai* dropped to 0.56 % and 0.48 % respectively. As for the Chinese kaolin, it had 1.37 % of Fe

before bioleaching and after treated with *B. cereus*, it was reduced to 0.80 % while the weight percentage of Chinese kaolin bioleached with *B. megaterium* and *B. aryabhattai* dropped to 0.62 % and 0.51 % respectively.

The effectiveness of the *Bacillus* bacteria in bioleaching could be calculated as the bioleaching efficiency using Equation 3.5, the bioleaching efficiency of *B. cereus*, *B. megaterium* and *B. aryabhattai* with Malaysian kaolin was found to be 57.4 %, 60.3 % and 65.9 % respectively as listed in Table 4.2. Apart from Malaysian kaolin, bioleaching efficiency of *B. cereus*, *B. megaterium* and *B. aryabhattai* with Chinese kaolin are also calculated and listed in Table 4.3 as 41.6 %, 54.7 % and 62.8 % respectively. The *B. aryabhattai* has the highest bioleaching efficiency for both the Malaysian kaolin and Chinese kaolin, resembling the phenanthroline analysis results. The experimental results concurred with a study done by Yap, et al. (2020) in which the kaolin bioleached with *B. cereus* strain had a 53.9 % bioleaching efficiency and a previous study by Jing, et al. (2021), in which the kaolin bioleached with *B. cereus* removed 38.7 %. The bioleaching efficiencies were able to be optimised to a slightly higher value than the results from previous bioleaching research of *B. cereus* with kaolin, which had an efficiency yield of 50 % to 53 % (Štyriaková & Štyriak, 2000). A study by Guo, et al. (2010) had a similar result of bioleaching efficiency on Chinese kaolin with a 45 % efficiency by using IRB. The slightly higher efficiency of the bioleaching could be due to the bioleaching were conducted by using the optimum glucose concentration. For instance, the glucose concentration used by Yap, et al. (2020) to achieve a 53.9 % bioleaching efficiency for Malaysian kaolin treated with *B. cereus* was 10 g/L. However, in the nutrient optimisation experiment it was found that bioleaching Malaysian kaolin with *B. cereus* at glucose concentration of 10 g/L had the lowest Fe(III) removal and the optimum glucose concentration was 8 g/L.

The Fe weight percentage of raw kaolin is close to the Fe weight percent of the abiotic control, which means the EDX results are reliable. The inconsistency of the results between the raw and control may be due to human error during the experiment. It could also be due to the small amount of kaolin sample used for analysis were taken from different portion of the whole dried kaolin powder which may result in having a certain degree of inconsistency as

the distribution of Fe in the kaolin dried powder is not homogeneous. The errors could be reduced by repeating the experiment with different portion of the kaolin sample to obtain an average Fe concentration.

Table 4.2: Weight percentage of each element in Malaysian kaolin.

	Wt %						Efficiency (%)
	O	Mg	Al	Si	K	Fe	
Raw	45.68	1.17	20.08	27.26	4.4	1.41	-
Control	48.07	1.57	18.77	25.51	4.56	1.52	-
B. cereus	49.03	0.98	19.74	26.03	3.62	0.60	57.4
B. megaterium	49.63	1.72	19.19	24.75	4.15	0.56	60.3
B. aryabhattai	50.49	1.77	19.22	24.17	3.87	0.48	65.9

Table 4.3: Weight percentage of each element in Chinese kaolin.

	Wt %						Efficiency (%)
	O	Mg	Al	Si	K	Fe	
Raw	46.06	0.4	23.49	27.13	1.55	1.37	-
Control	46.77	0.51	20.1	31.11	0.53	0.98	-
B. cereus	50.59	0.65	21.44	25.26	1.26	0.80	41.6
B. megaterium	50.34	0.23	22.26	25.84	0.71	0.62	54.7
B. aryabhattai	50.35	0.63	20.1	27.68	0.73	0.51	62.8

4.7 XRD spectra of Malaysian and Chinese kaolin

The XRD results of both Malaysian and Chinese kaolin has several peaks such as the angles 12°, 25° and 27° that characterize the kaolinite were detected (Daou, et al, 2020; Xue, et al., 2023). The XRD pattern from the analysis post little to no mineral composition changes or structural changes in both the Malaysian and Chinese kaolin as the peaks coincides as shown in Figure 4.15 and Figure 4.16. The same results were observed by Győrfi, et al. (2020) in which there is negligible changes in the peak positions, the kaolinite structure was not affected by Fe minerals removal. This results are also in agreement with a study by Li, et al. (2015) in which the structure of kaolins was maintained. There is also no formation of secondary minerals from the XRD

results as the peaks are all in the same angles. However, there are different intensities of diffraction lines identified for Malaysian kaolin at 12°, 25°, 27°, 38° and 46°. Similarly, for Chinese kaolin at 12°, 25°, 27°, 38° and 62° has different intensities. The intensities of the peaks of Malaysian kaolin treated with *B. cereus* and *B. megaterium* is higher than the untreated Malaysian kaolin as shown in Figure 4.15a and Figure 4.15b respectively whereas the intensities of Malaysian kaolin treated with *B. aryabhattai* is lower than untreated Malaysian kaolin as shown in Figure 4.15c. But for Chinese kaolin, all the bioleached kaolin XRD pattern in Figure 4.16a, Figure 4.16b and Figure 4.16c has lower intensities as compared to untreated Chinese kaolin. The different intensities could be inferred as the change of crystallite size, the decrease of the mean lattice strain (Kumar, Panda and Singh, 2013) and having different amount of clay minerals in the Malaysian and Chinese kaolin before and after bioleaching. The other low intensity or less pronounced asymmetry of the peaks were likely a result of the disorder of the kaolin structure (Senoussi, et al., 2016).

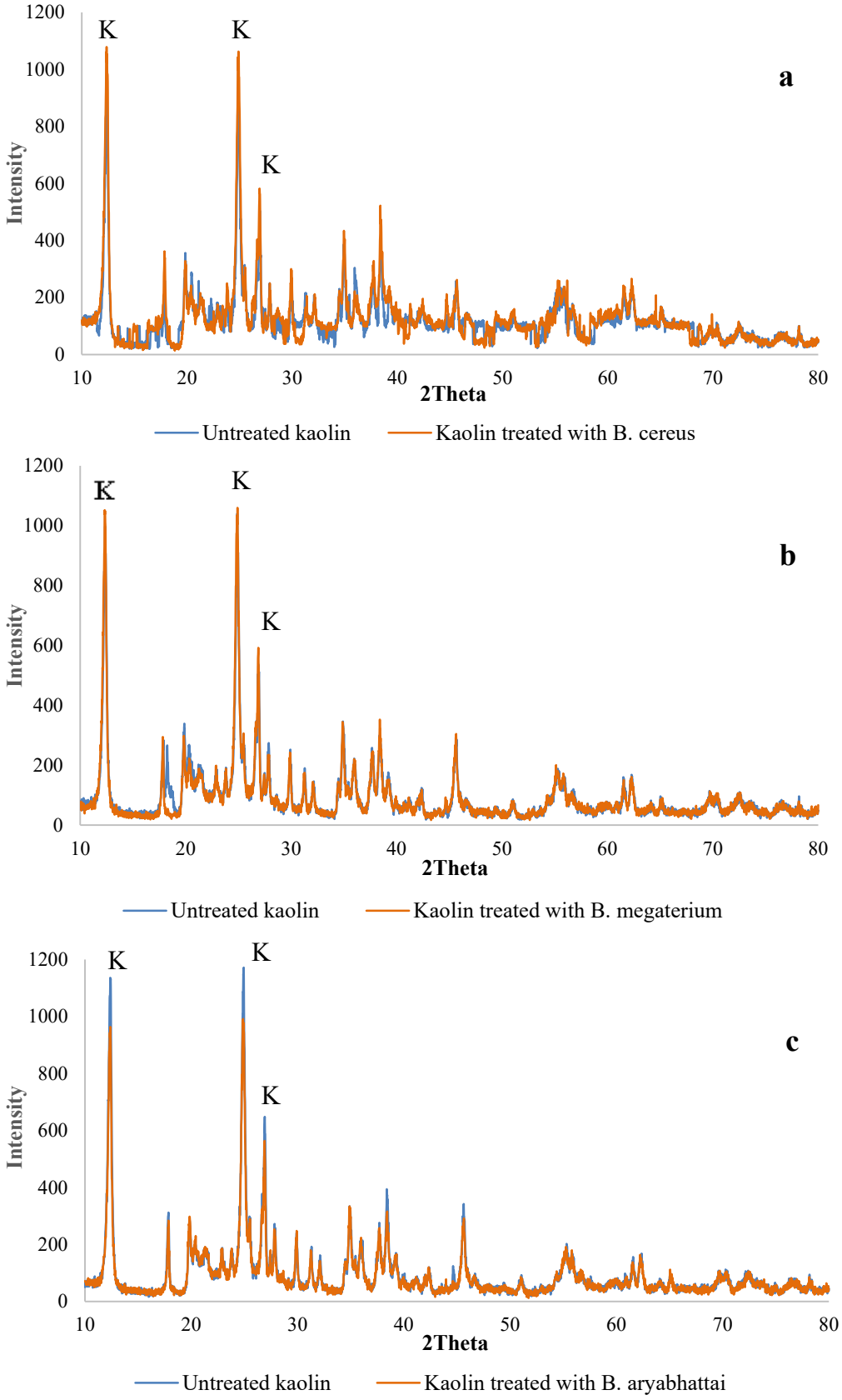

Figure 4.15: XRD patterns of Malaysian kaolin before and after (a) bioleached with *B. cereus*, (b) bioleached with *B. megaterium* and (c) bioleached with *B. aryabhattai*.

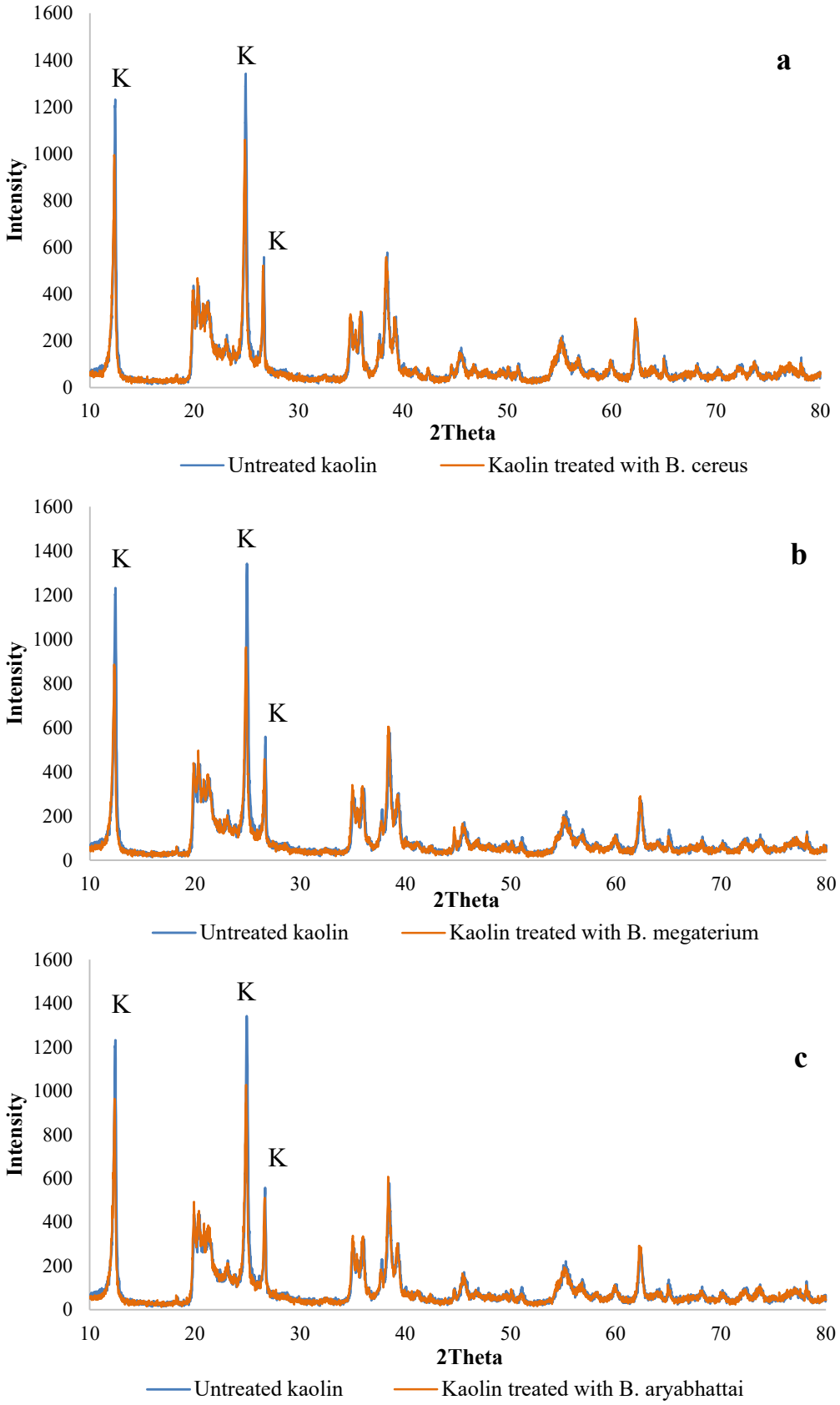

Figure 4.16: XRD patterns of Chinese kaolin before and after (a) bioleached with *B. cereus*, (b) bioleached with *B. megaterium* and (c) bioleached with *B. aryabhattai*.

4.8 FTIR results before and after bioleaching

From the FTIR results before bioleaching took place, there were 2 bands that was identified from the wavenumbers generated. Each band is associated with one hydroxyl group of the kaolinite structure (Van der Marel and Zwiers, 1959). Based on previous studies, there are usually 4 O-H bands in kaolin which are 3695 cm^{-1}, 3670 cm^{-1}, 3650 cm^{-1} and 3620 cm^{-1} (Kloprogge, 2019) but occasionally there is a fifth band at around 3686 cm^{-1} in the presence of transverse optical (TO) and longitudinal optical (LO) vibrations (Farmer, 2000). The identified bands of Malaysian kaolin before bioleaching were 3689 cm^{-1} and 3618 cm^{-1} as shown in Figure 4.17. While the raw Chinese kaolin FTIR peaks that was identified in Figure 4.18 were 3687 cm^{-1} and 3618 cm^{-1}. The 3689 cm^{-1} band of Malaysian kaolin and the 3687 cm^{-1} band of Chinese kaolin was identified as the fifth band, interpreted as the TO mode relating to the in-phase OH stretching vibration. The fifth band has different intensities depending on the nature and origin of the clay (Johnston, et al., 1985). An uncoupled inner surface hydroxyl stretching mode will cause the occurrence of this band (Michaelian, et al., 1987). Moreover, the 3618 cm^{-1} FTIR band of both the Malaysian and Chinese kaolin is identified as related to the 3620 cm^{-1} band, interpreted as the inner hydroxyl group pointing towards the tetrahedral sheet (Kloprogge, 2019). Although kaolinites usually show four bands, 3670 cm^{-1} and 3652 cm^{-1} bands of less ordered kaolinite were very poorly developed and in some cases only a single band was observed at 3652 cm^{-1} (Van der Marel and Krohmer, 1969). There are only 2 bands from the experimental FTIR results because bands at around 3693 cm^{-1} and 3620 cm^{-1} are sharp and intense although each samples has different relative intensities. In this particular experiment, both the 3670 cm^{-1} and 3650 cm^{-1} bands were not visible in the results which revealed that the Malaysian and Chinese kaolin used are less ordered kaolin.

FTIR spectra of the Malaysian and Chinese kaolin after bioleaching is very similar to the raw Malaysian and Chinese kaolin. The Malaysian kaolin has the same observed bands of 3689 cm^{-1} and 3618 cm^{-1} after bioleaching with *B. cereus*, *B. megaterium* and *B. aryabhattai* as indicated in Figure 4.19, Figure 4.20 and Figure 4.21 respectively. The Chinese kaolin also has the

observed bands of 3688-3689 cm^{-1} which is very close to the untreated Chinese kaolin 3687 cm^{-1} and 3618 cm^{-1} band as shown in Figure 4.22, Figure 4.23 and Figure 4.24 respectively. This indicates that the bioleaching of both the Malaysian and Chinese kaolin does not affect the observed bands since the bands are very similar before and after bioleaching. A previous study also had similar observation, the surface modified kaolin did not change the FTIR peaks and it was suggested that the basic crystal structure of kaolinite remained constant (Li, et al, 2015).

Other than the 5 common bands that are usually found in kaolin, there are also the 1113 cm^{-1} band in both untreated and treated Malaysian and Chinese kaolin that are identified as the 1115 cm^{-1} band that was assigned to the apical Si-O stretching vibration. Furthermore, the 909-910 cm^{-1} band of the Malaysian and Chinese kaolin was identified as the 915 cm^{-1} band assigned to the vibration of inner Al–OH groups (Li, et al, 2015; Mbey, et al., 2019).

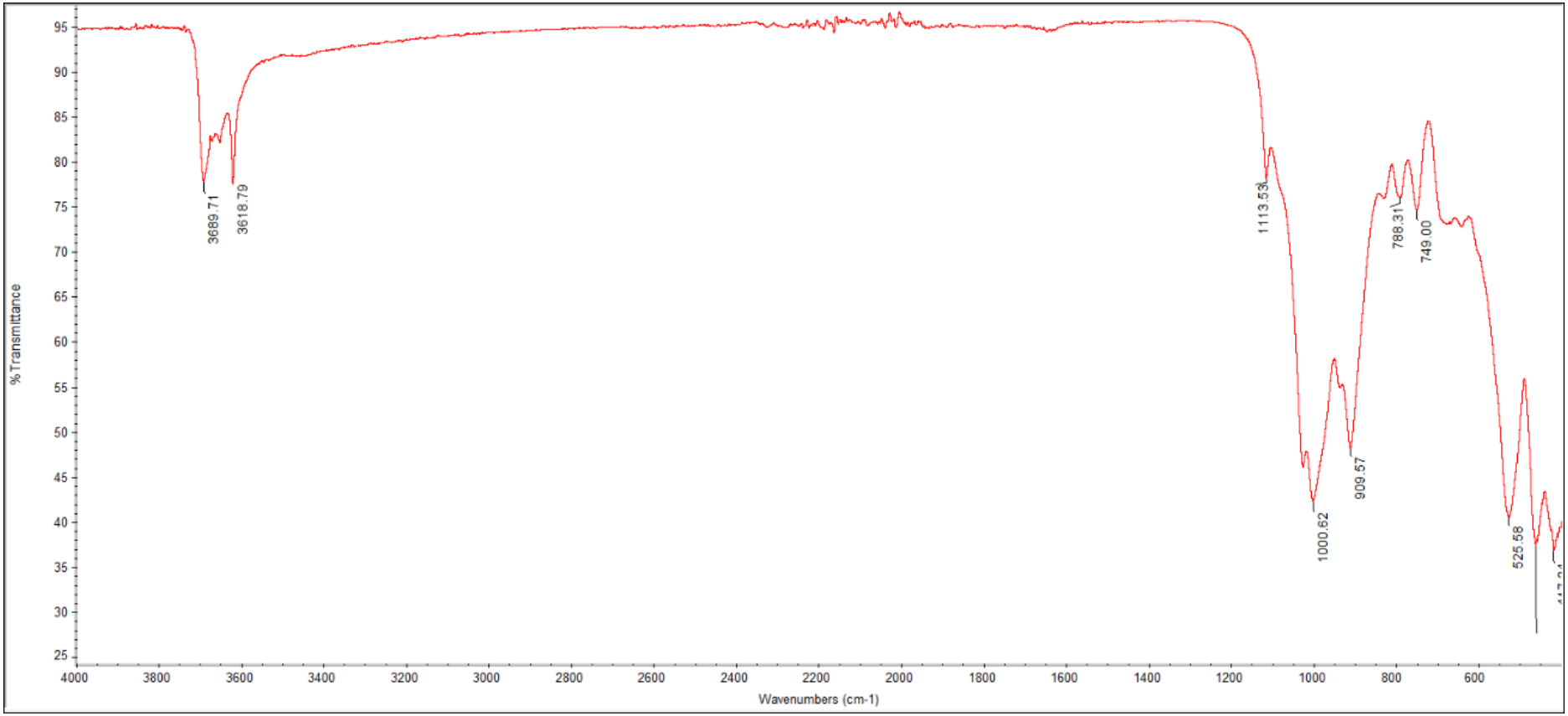

Figure 4.17: FTIR spectrum of raw Malaysian kaolin.

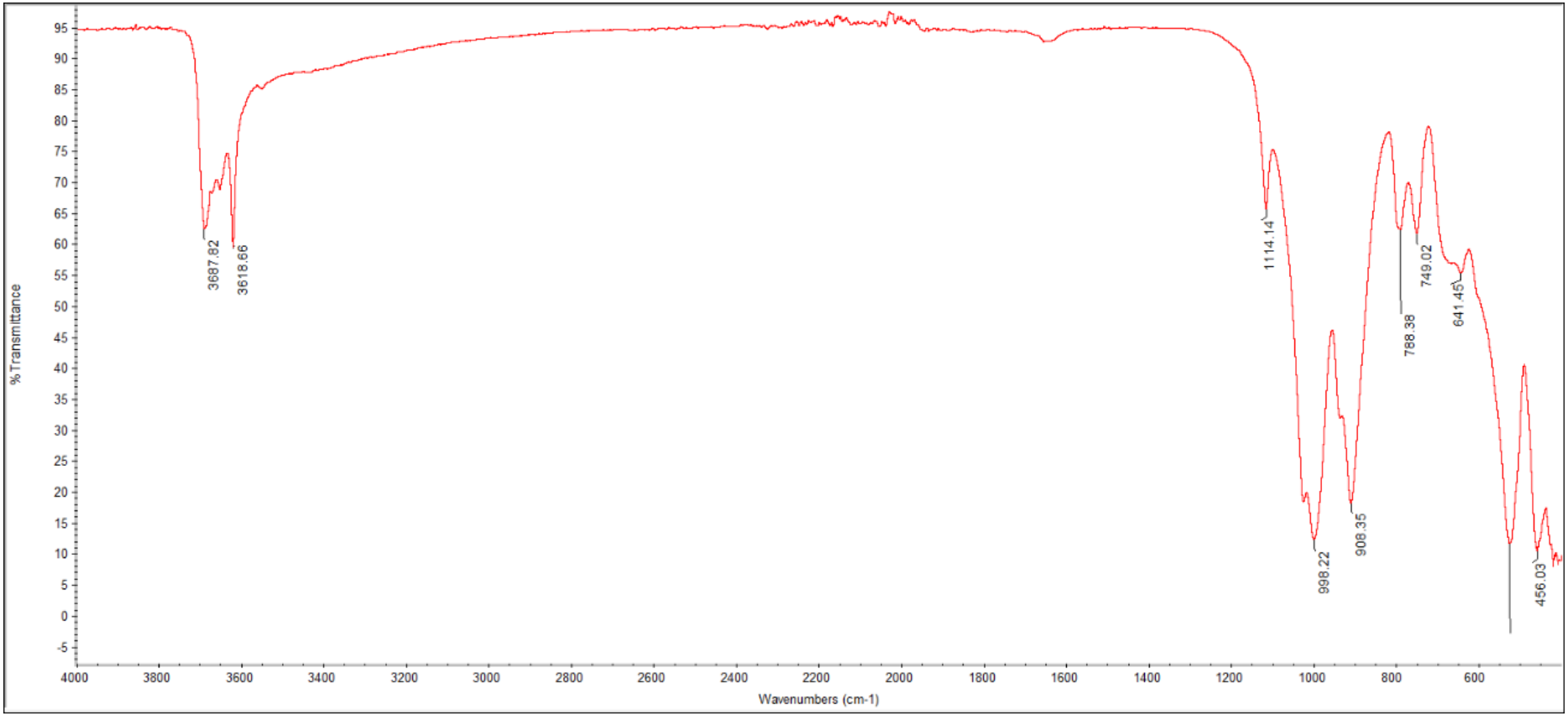

Figure 4.18: FTIR spectrum of raw Chinese kaolin.

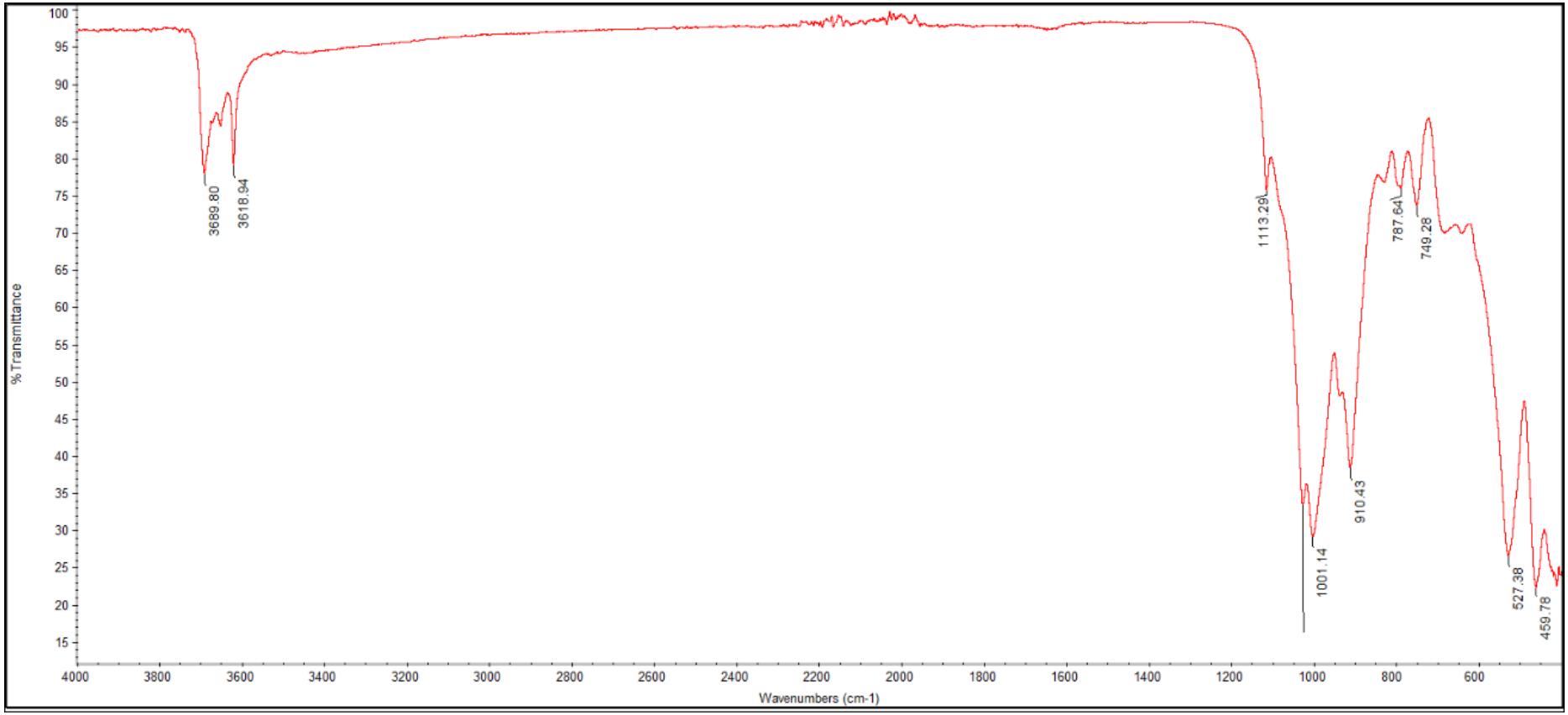

Figure 4.19: FTIR spectrum of Malaysian kaolin treated with *B. cereus*.

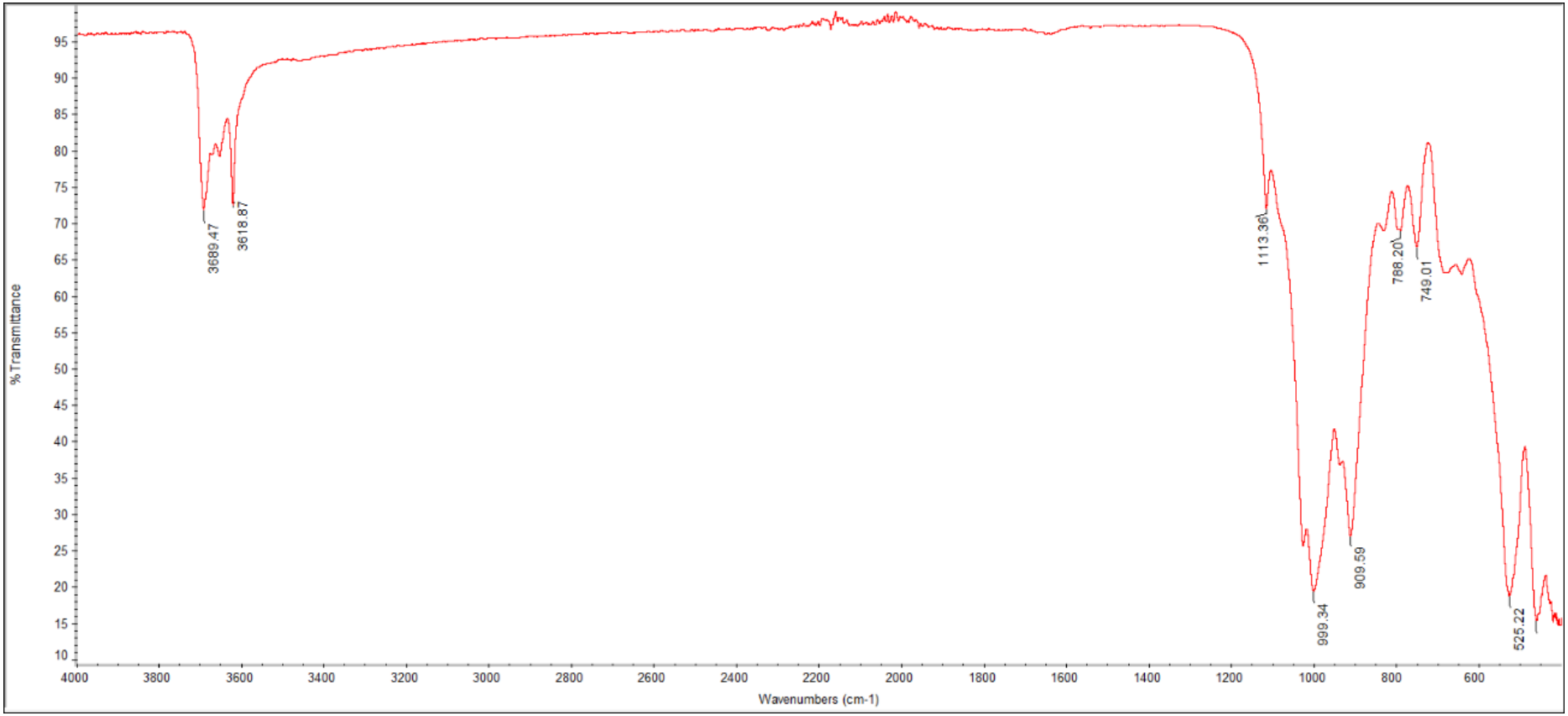

Figure 4.20: FTIR spectrum of Malaysian kaolin treated with *B. megaterium*.

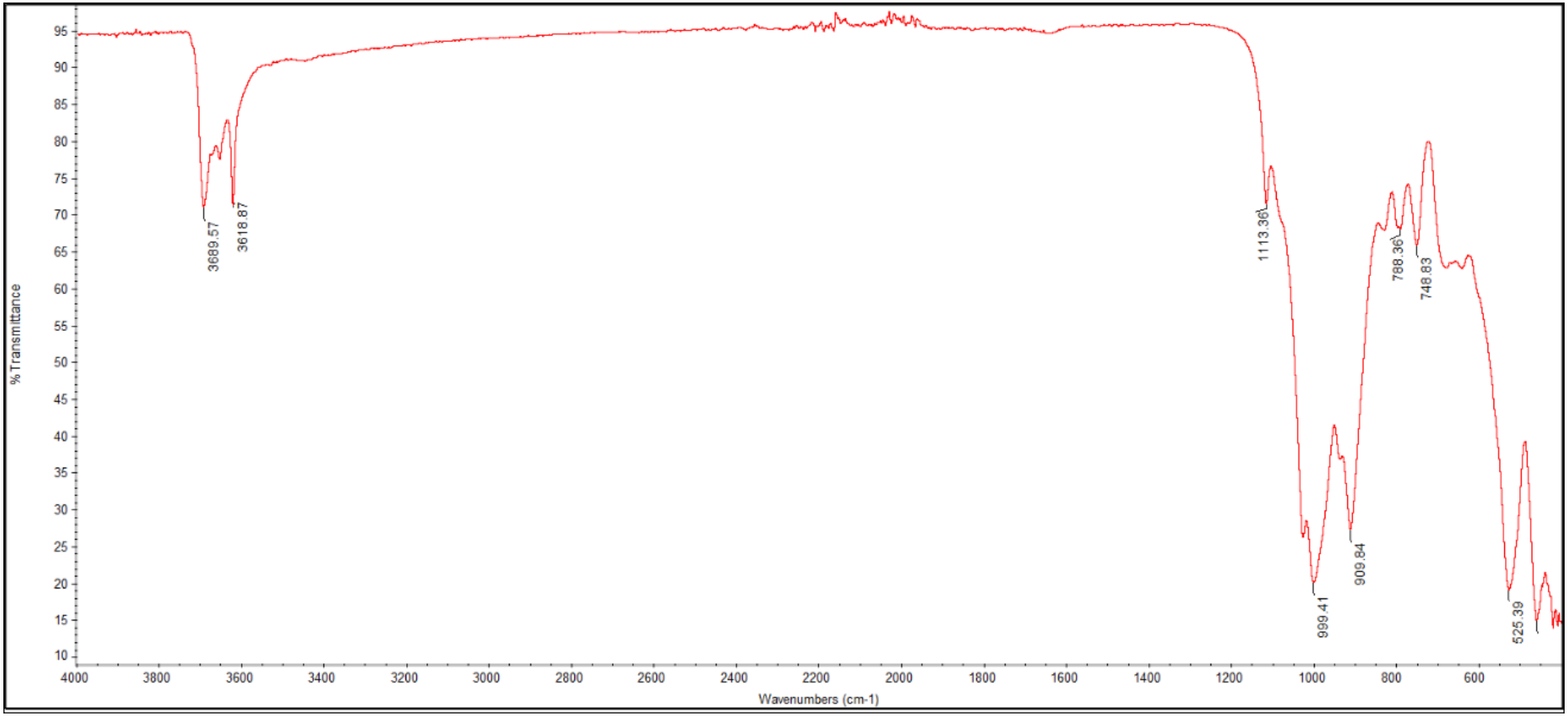

Figure 4.21: FTIR spectrum of Malaysian kaolin treated with *B. aryabhattai*.

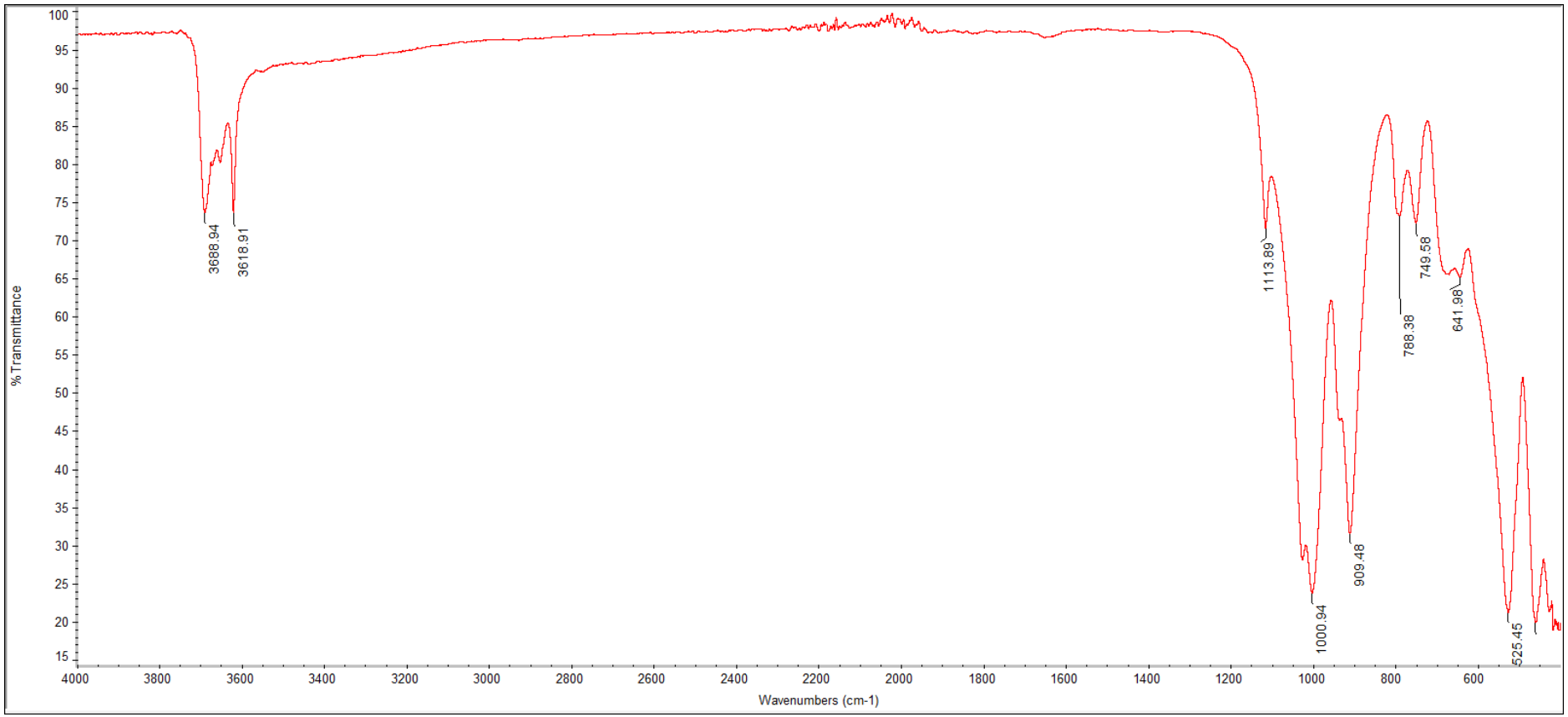

Figure 4.22: FTIR spectrum of Chinese kaolin treated with *B. Cereus*.

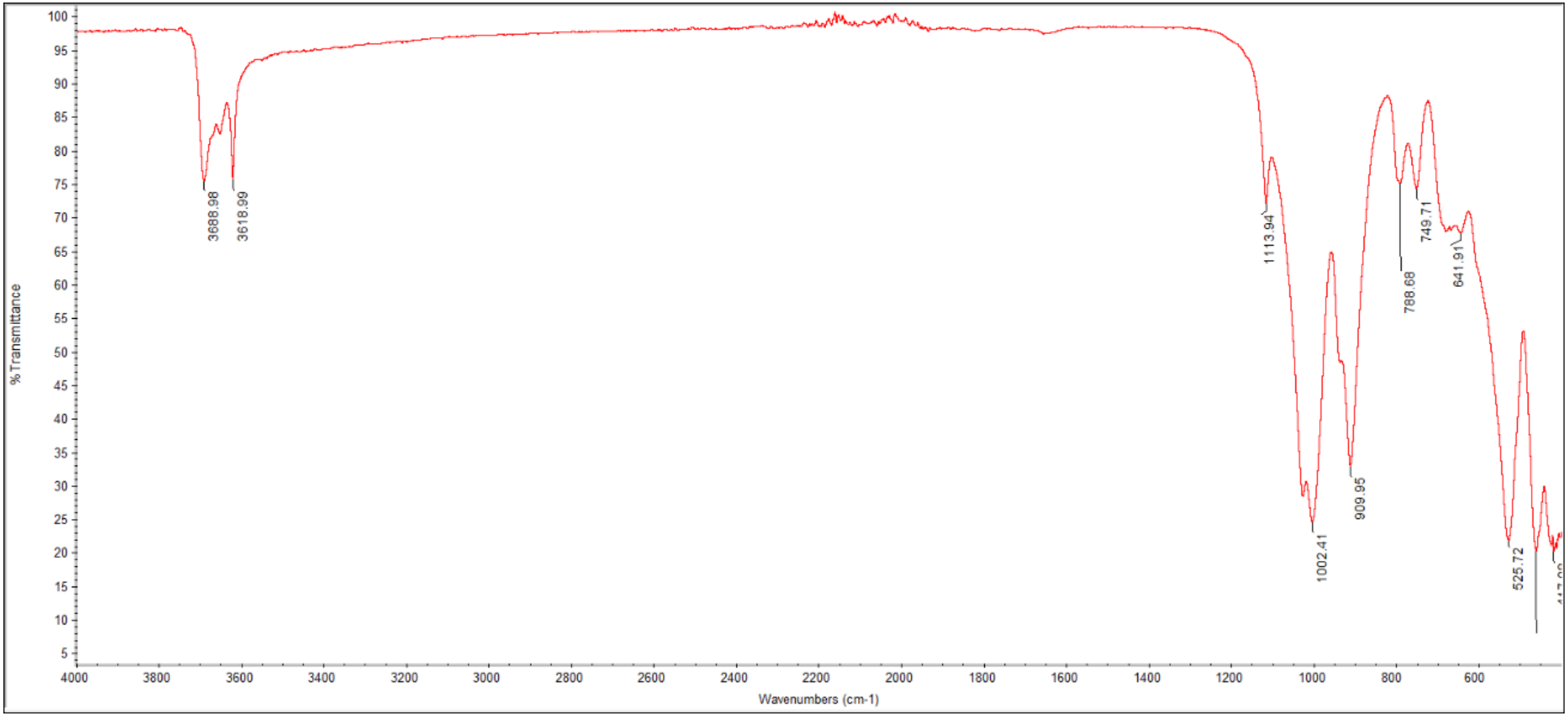

Figure 4.23: FTIR spectrum of Chinese kaolin treated with *B. megaterium*.

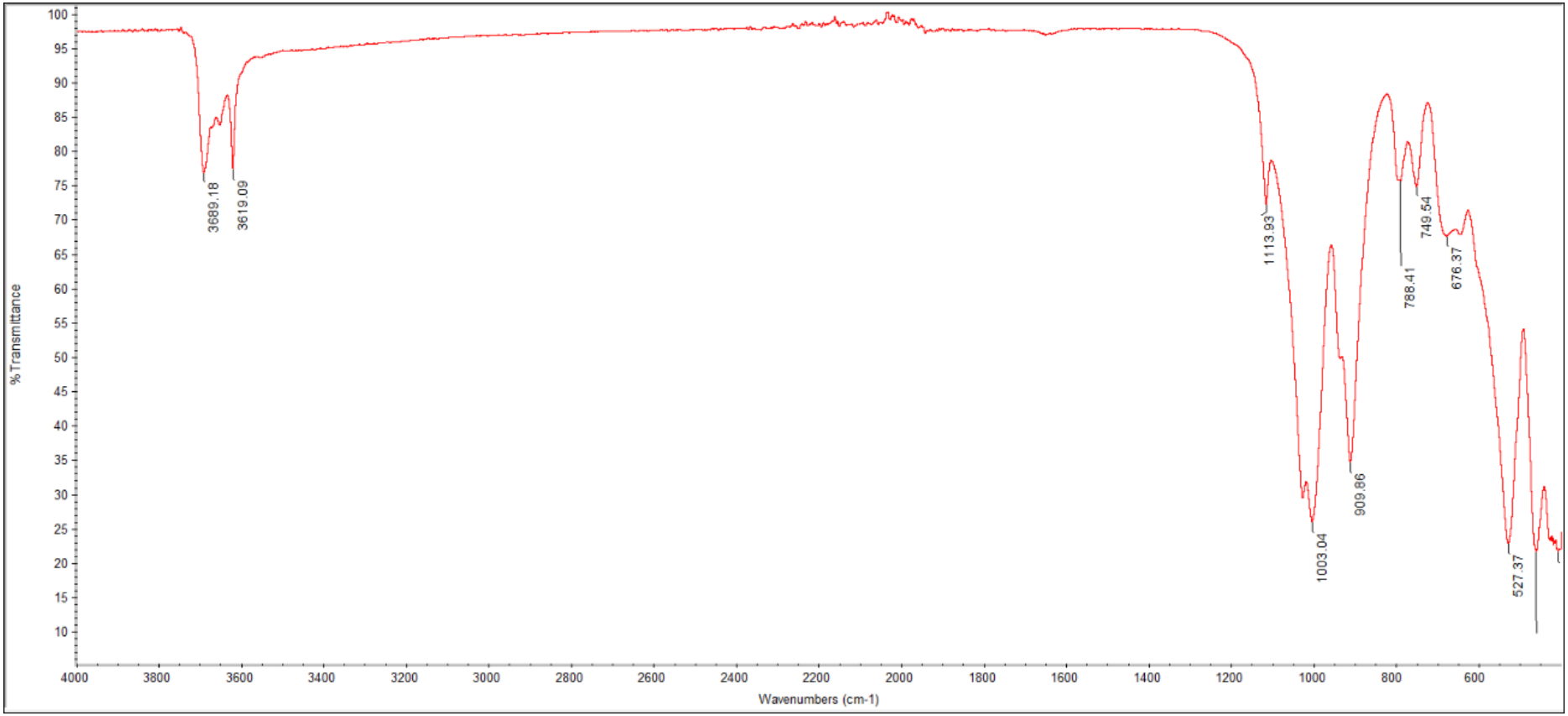

Figure 4.24: FTIR spectrum of Chinese kaolin treated with *B. aryabhattai*

4.9 Summary

In short, morphological changes were observed in the Malaysian and Chinese kaolin after treatment with *Bacillus* spp. bacteria through bioleaching but the bonds of both Malaysian and Chinese kaolin remained the same as revealed in the SEM and FTIR analysis. There is a significant reduction in Fe weight percentage observed across several analytical techniques before and after bioleaching for all three bacteria species. Reduction of Fe was affirmed in the phenanthroline analysis, ICP-OES and EDX analysis. The difference between the bioleaching efficiency of ICP-OES analysis results and EDX analysis results may be due to the sensitivity of the technique as well as Fe distribution in the kaolin sample tested. Generally, ICP-OES analysis has a higher accuracy because the EDX analysis can only analyse a sample area as large as the size of the electron beam, only local concentrations of sample taken into account and distribution of Fe on kaolin surface is not homogenous by nature but an ICP-OES analysis can identify an average concentration of the sample because the samples are mixed evenly and dissolved with acid (Michalak, Chojnacka and Marycz, 2010). Lastly, XRD analysis revealed that the mineralogy of kaolin was not altered by bioleaching.

CHAPTER 5

CONCLUSIONS AND RECOMMENDATIONS

5.1 Conclusions

This study analysed the morphological, chemical and structural changes of kaolin bioleaching using *Bacillus* species. From the analysis of the experimental results, the objective of the experiment was achieved as it was found in phenanthroline analysis that the optimum nutrients condition for bioleaching kaolin with *B. cereus* is 6 g/L of glucose concentration with Fe(II) concentration of 1.7 µg/mL on day 5 while for *B. megaterium* and *B. aryabhattai* the optimum glucose concentration is 10 g/L with highest Fe(II) concentration of 1.63 µg/mL and 1.57 µg/mL respectively.

The objective to measure the Fe reduction ability of *Bacillus* bacteria was also achieved as reduction of Fe was clearly visible in phenanthroline analysis and ICP-OES analysis whereby the Fe(II) concentration increase during the period of 10 days of bioleaching. The EDX analysis revealed that the bioleaching efficiency was slightly higher than the previous studies as Malaysian kaolin treated with *B. cereus*, *B. megaterium* and *B. aryabhattai* was found to be 57.4 %, 60.3 % and 65.9 % respectively. Whereas for Chinese kaolin treated with *B. cereus*, *B. megaterium* and *B. aryabhattai*, the bioleaching efficiency was found to be 41.6 %, 54.7 % and 62.8 % respectively. Optimum glucose concentration used for the bioleaching experiment could be the contributing factor to the small increase in the bioleaching efficiency.

From the analysis, it was obvious that the Malaysian and Chinese kaolin experienced changes in terms of structure and surface morphology after bioleaching with *Bacillus* spp. bacteria. From the SEM analysis, it was revealed that the surface structure of both Malaysian and Chinese kaolin increased in crystallinity. The chemical composition and bonds of both Malaysian and Chinese kaolin remains unchanged after bioleaching as determined in the similar 12°, 25°, 27° and 38° peaks of XRD analysis as well

as the 3620 cm^{-1} and 3686 cm^{-1} bands of FTIR analysis. Therefore, the third objective was also achieved in this project.

Bioleaching of kaolin could be applied in the industry by mixing the kaolin powder in water with active IRB and nutrients solution in a bioleaching reactor. The results of this study can be used to scale-up the bioleaching process to industrial scale once a meaningful and feasible percentage Fe reduction is achieved (>80% Fe reduction). Further optimisation of the process on a laboratory scale will be useful to render scaling-up a reality.

5.2 Recommendations for future work

Several improvements can be recommended for future studies of bioleaching. Due to time constraints, it was not possible to try the acid digestion with different strong acids to determine the suitable acid for complete digestion of kaolin. Since kaolin contains silica, it will only be fully digested in hydrofluoric (HF) acid. However, HF acid is very corrosive, highly toxic and will dissolve the glassware available. Hence, it is prohibited in laboratory and instead of using HF acid, sulphuric acid was used. The ICP-OES analysis could be improved by using a two stage acid digestion with strong concentrated acid such as nitric acid and sulphuric acid.

Future work could aim to get consistent results of bioleaching efficiency between the ICP-OES analysis and EDX analysis, more experiments with an improved ICP-OES analysis using a more suitable acid or the suggested two-stage acid digestion method might yield a consistent bioleaching efficiency result.

Furthermore, other parameters such as pH condition and cell adaptation could be optimised to improve the bioleaching efficiency to achieve a higher Fe reduction within a shorter period of time. From optimising various parameters from laboratory scale, the data will be useful in scaling up to industrial scale bioleaching. With the implementation of bioreactor, multiple parameters will be able to be controlled at the same time under controlled condition. For ease of quality control and monitoring, batch process will be preferred before scaling up to a faster pace using continuous process.

REFERENCES

Abdel-Khalek, N. A., Selim, K. A., Abdallah, S. S. and Yassin, K. E., 2013. Bioflotation of low Grade Egyptian Iron ore using *Brevundimonas diminuta* Bacteria: Phosphorus removal. *Elixir International Journal*, 63, pp.18666-18670.

Abdel-Shafi, S., Reda, F. M. and Ismail, M., 2017. Production of Terpenoids, Terpene Alcohol, Fatty Acids and N_2 Compounds by Bacillus amyloliquefaciens S5i4 Isolated from Archaeological Egyptian Soil. *Advanced Techniques in Clinical Microbiology*, [online] 1(3). Available at: https://www.imedpub.com/articles/production-of-terpenoids-terpene-alcoholfatty-acids-and-n2-compounds-by-bacillusamyloliquefaciens-s5i4-isolated-fromarchaeological.php?aid=20888 [Accessed 11 September 2022].

Abdullahi, T., Harun, Z. and Othman, M. H. D., 2017. A review on sustainable synthesis of zeolite from kaolinite resources via hydrothermal process. *Advanced Powder Technology*, 28(8), pp.1827-1840.

Adekola, F. A., Baba, A. A. and Girigisu, S., 2017. Dissolution kinetics of kaolin mineral in acidic media for predicting optimal condition for alum production. *Journal of Central South University*, 24(2), pp.318–324. doi:https://doi.org/10.1007/s11771-017-3433-9.

Arslan, V., 2021. A study on the dissolution kinetics of iron oxide leaching from clays by oxalic acid. Physicochemical Problems of Mineral Processing, [e-journal] 57(3), pp.97–111. https://doi.org/10.37190/ppmp/135749.

Arslan, V. and Bayat, O., 2009. Removal of Fe from kaolin by chemical leaching and bioleaching. *Clays and Clay Minerals*, [e-journal] 57(6), pp.787–794. https://doi.org/10.1346/CCMN.2009.05706011.

Blodau, C. and Gatzek, C., 2006. Chemical controls on iron reduction in schwertmannite-rich sediments. *Chemical Geology*, [e-journal] 235(3-4), pp.366–376. https://doi.org/10.1016/j.chemgeo.2006.08.003.

Brindley, G. W., 1955. The Structure and morphology of a kaolin clay from Les Eyzies (France) 1. *Clays and Clay Minerals*, 4(1), pp.61–66. doi:https://doi.org/10.1346/ccmn.1955.0040109.

Buyondo, K. A., Kasedde, H. and Kirabira, J. B., 2022. A comprehensive review on kaolin as pigment for paint and coating: Recent trends of chemical-based paints, their environmental impacts and regulation. *Case Studies in Chemical and Environmental Engineering*, [e-journal] 6. https://doi.org/10.1016/S0169-1317(02)00111-4.

Cameselle, C., Ricart, M. T., Núñez, M. J. and Lema, J. M., 2003. Iron removal from kaolin. Comparison between ‘in situ’ and ‘two-stage’

bioleaching processes. *Hydrometallurgy*, [e-journal] 68(1-3), pp.97–105. http://dx.doi.org/10.1016/S0304-386X(02)00196-2.

Daou, I., Lecomte-Nana, G. L., Tessier-Doyen, N., Peyratout, C., Gonon, M. and Guinebretière, R., 2020. Probing the dehydroxylation of kaolinite and Halloysite by In Situ High Temperature X-ray Diffraction. *Minerals*, [e-journal] 10(5), pp.480–480. doi:https://doi.org/10.3390/min10050480.

Dong, H. (2012). Clay-Microbe interactions and implications for environmental mitigation. *Elements*, [e-journal] 8(2), pp.113-118.https://doi.org/10.2113/gselements.8.2.113.

Fakharpour, M. and Hajihoseini, J., 2021. Optimal removal of iron impurities from kaolin by combination of *Aspergillus niger* & *Bacillus subtilis*. *International Journal of Materials Research*, [e-journal] 112(6), pp.498-504. https://doi.org/10.1515/ijmr-2020-8048.

Farmer, V. C., 2000. Transverse and longitudinal crystal modes associated with OH stretching vibrations in single crystals of kaolinite and dickite. *Spectrochimica Acta Part A: Molecular and Biomolecular Spectroscopy*, 56(5), pp.927–930. doi:https://doi.org/10.1016/s1386-1425(99)00182-1.

Finck, N., Schlegel, M. L. and Bauer, A., 2015. Structural iron in dioctahedral and trioctahedral smectites: a polarized XAS study. *Physics and Chemistry of Minerals*, [e-journal] 42(10), pp.847–859. https://doi.org/10.1007/s00269-015-0768-3.

Gougazeh, M., 2018. Removal of iron and titanium contaminants from Jordanian Kaolins by using chemical leaching. *Journal of Taibah University for Science*, [e-journal] 12(3), pp.247–254. https://doi.org/10.1080/16583655.2018.1465714.

Guo, M., Lin, Y., Xu, X. and Chen, Z., 2010. Bioleaching of iron from kaolin using Fe(III)-reducing bacteria with various carbon nitrogen sources. *Applied Clay Science*, [e-journal] 48(3), pp.379–383. http://dx.doi.org/10.1016/j.clay.2010.01.010.

Guo, M. R., He, Q. X., Li, Y. M., Lu, X. and Chen, Z., 2010. Removal of Fe from kaolin using dissimilatory Fe(III)-Reducing Bacteria. *Clays and Clay Minerals*, [e-journal] 58(4), pp.515–521. https://doi.org/10.1346/CCMN.2010.0580406.

Győrfi, K., Vágvölgyi, V., Zsirka, B., Horváth, E., Szilágyi, R. K., Baán, K., Balogh, S. and Kristóf, J., 2020. Kaolins of high iron-content as photocatalysts: Challenges of acidic surface modifications and mechanistic insights. *Applied Clay Science*, [e-journal] 195, p.105722. doi:https://doi.org/10.1016/j.clay.2020.105722.

He, Q., Huang, X. and Chen, Z., 2011. Influence of organic acids, complexing agents and heavy metals on the bioleaching of iron from kaolin using Fe(III) - reducing bacteria. *Applied Clay Science*, [e-journal] 51(4), pp.478–483. https://doi.org/10.1016/j.clay.2011.01.012.

Hernández, R. A., García, F. L., Cruz, L. E. H. and Luévanos, A. M., 2013. *Iron removal from a kaolinitic clay by leaching to obtain high whiteness index*. In: IOP Science, IOP Conference Series: Materials Science and Engineering. Yucatan, Mexico, 27 February to 2 March 2012.

Hosseini, M. R. and Ahmadi, A., 2015. Biological beneficiation of kaolin: A review on iron removal. *Applied Clay Science*, 107, pp.238–245.

Hosseini, M. R., Pazouki, M., Ranjbar, M. and Habibian, M., 2007. Bioleaching of iron from highly contaminated Kaolin clay by Aspergillus niger. *Applied Clay Science*, [e-journal] 37(3-4), pp.251–257. https://doi.org/10.1016/j.clay.2007.01.010.

Huang, T., Lei, S. M., Liu, Y. Y. and Li, B., 2019. Optimization for the COD reduction and thermodynamics research of coalseries kaolin. *Environmental Earth Sciences*, [e-journal] 78(363). https://doi.org/10.1007/s12665-019-8363-4.

Hubadillah, S. K., Othman, M. H. D., Matsuura, T., Ismail, A. F., Rahman, M. A., Harun, Z., Jaafar, J. and Nomura, M., 2018. Fabrications and applications of low cost ceramic membrane from kaolin: A comprehensive review. *Ceramics International*, 44(5), pp.4538-4560.

Hussain, Z., Grimes, S., Shahid, M., Bukhari, S. A., Raza Naqvi, S. A., Pirzada, T. and Zia, S., 2013. Leaching of Copper Secondary Wastes: Possible Soil Contaminants. *Asian Journal of Chemistry*, [e-journal] 25(7), pp.4051–4054. http://dx.doi.org/10.14233/ajchem.2013.13957.

Johnston, C. T., Sposito, G., Birge, R. R., 1985. Raman Spectroscopic Study of Kaolinite in Aqueous Suspension. *Clays and Clay Minerals*, [e-journal] 33(6), pp.483–489. doi:https://doi.org/10.1346/ccmn.1985.0330602.

Jing, H., Liu, Z., Kuan, S. H., Chieng, S. and Ho, C. L., 2021. Elucidation of Gram-Positive Bacterial Iron(III) Reduction for Kaolinite Clay Refinement. *Molecules*, [e-journal] 26(11), p.3084. https://doi.org/10.3390/molecules26113084.

Kaksonen, A. H., Boxall, N. J., Gumulya, Y., Khaleque, H. N., Morris, C., Bohu, T., Cheng, K. Y., Usher, K. M. and Lakaniemi, A., 2018. Recent progress in biohydrometallurgy and microbial characterisation. *Hydrometallurgy*, 180, pp.7-25.

Kappler, A., Wuestner, M. L., Ruecker, A., Harter, J., Halama, M. and Behrens, S., 2014. Biochar as an Electron Shuttle between Bacteria and Fe(III)

Minerals. *Environmental Science & Technology Letters*, [e-journal] 1(8), pp.339–344. https://doi.org/10.1021/ez5002209.

Kloprogge, J., 2019. The Kaolin Group: Hydroxyl Groups. *Springer mineralogy*, [e-journal], pp.41–96. doi:https://doi.org/10.1007/978-3-030-02373-7_3.

Koo, T., Jang, Y., Kogure, T., Kim, J. H., Park, B. C., Sunwoo, D. and Kim, J., 2014. Structural and chemical modification of nontronite associated with microbial Fe(III) reduction: Indicators of 'illitization'. *Chemical Geology*, [e-journal] 377, pp.87–95. doi:https://doi.org/10.1016/j.chemgeo.2014.04.005.

Kumar, S., Panda, A. K. and Singh, R. K., 2013. Preparation and Characterization of Acid and Alkaline Treated Kaolin Clay. *Bulletin of Chemical Reaction Engineering & Catalysis*, [e-journal] 8(1), pp.61-69. https://doi.org/10.9767/bcrec.8.1.4530.61-69.

Lee, E. Y., Cho, K. S. and Ryu, H. W., 2002. Microbial refinement of kaolin by iron-reducing bacteria. *Applied Clay Science*, 22(1-2), pp.47-53.

Lee, S. O., Tran, T., Park, Y. Y., Kim, S. J. and Kim, M. J., 2006. Study on the kinetics of iron oxide leaching by oxalic acid. *International Journal of Mineral Processing*, [e-journal] 80(2), pp.144–152. https://doi.org/10.1016/j.minpro.2006.03.012.

Li, X., Ouyang, J., Zhou, Y. and Yang, H., 2015. Assembling strategy to synthesize palladium modified kaolin nanocomposites with different morphologies. *Scientific Reports*, [e-journal] 5(1). doi:https://doi.org/10.1038/srep13763.

Mbey, J. A., Thomas, F., Razafitianamaharavo, A., Caillet, C. and Villiéras, F., 2019. A comparative study of some kaolinites surface properties. *Applied Clay Science*, [e-journal] 172, pp.135–145. doi:https://doi.org/10.1016/j.clay.2019.03.005.

Michaelian, K. H., Bukka, K. and Permann, D. N. S., 1987. Photoacoustic infrared spectra (250–10 000 cm^{-1}) of partially deuterated kaolinite # 9. *Canadian journal of chemistry*, *65*(6), pp.1420-1423.

Michalak, I., Chojnacka, K. and Marycz, K., 2010. Using ICP-OES and SEM-EDX in biosorption studies. *Microchimica Acta*, [e-journal] 172(1-2), pp.65–74. doi:https://doi.org/10.1007/s00604-010-0468-0.

Murray, H. H., 2006. Chapter 5 Kaolin Applications. *Developments in Clay Science*, 2, pp.85-109.

Mhete, M., Eze, P. N., Rahube, T. O. and Akinyemi, F. O., 2020. Soil properties influence bacterial abundance and diversity under different land-use regimes in semi-arid environments. *Scientific African*, [e-journal] 7, p.e00246. https://doi.org/10.1016/j.sciaf.2019.e00246.

Natarajan, K. A., 2018. Microbially Induced Mineral Beneficiation. *Biotechnology of Metals*, [e-journal] pp.243–304. https://doi.org/10.1016/B978-0-12-804022-5.00010-4.

Peng, T., Zhou, D., Liu, Y., Yu, R., Qiu, G. and Zeng, W., 2019. Effects of pH value on the expression of key iron/sulfur oxidation genes during bioleaching of chalcopyrite on thermophilic condition. *Annals of Microbiology*, [e-journal] 69(6), pp.627–635. https://doi.org/10.1007/s13213-019-01453-y.

Puglisi, E., Romaniello, F., Galletti, S., Boccaleri, E., Frache, A. and Cocconcelli, P. S., 2019. Selective bacterial colonization processes on polyethylene waste samples in an abandoned landfill site. *Scientific Reports*, [e-journal] 9(1), p.14138. https://doi:10.1038/s41598-019-50740-w.

Roy, J. J., Madhavi, S. and Cao, B., 2021. Metal extraction from spent lithium-ion batteries (LIBs) at high pulp density by environmentally friendly bioleaching process. *Journal of Cleaner Production*, [e-journal] 280(2). https://doi.org/10.1016/j.jclepro.2020.124242.

Ribeiro, F. R., Filho, F. B. E., Fabris, J. D., Mussel, W. N. and Novais, R. F., 2007. POTENTIAL USE OF A CHEMICAL LEACHING REJECT FROM A KAOLIN INDUSTRY AS AGRICULTURAL FERTILIZER. *Revista Brasileira de Ciência do Solo,* [e-journal] 31(5), pp.939–946. http://dx.doi.org/10.1590/S0100-06832007000500011.

Saeid, A., Prochownik, E. and Dobrowolska-Iwanek, J., 2018. Phosphorus Solubilization by Bacillus Species. *Molecules*, [e-journal] 23(11), p.2897. https://doi.org/10.3390/molecules23112897.

Sánchez-Palencia, Y., Bolonio, D., Ortega, M. F., García-Martínez, M. J., Ortiz, J. E., Rayo, F., Arregui, L., Serrano, S., Llamas, J. F. and Canoira, L., 2022. Iron Removal from Kaolin Waste Dumps by Chemical (Oxalic and Citric Acids) and Biological (*Bacillus* Strain) Leaching. *Clays Clay Miner*, [e-journal] 70, pp.386-404. https://doi.org/10.1007/s42860-022-00192-7.

Seabaugh, J. L., Dong, H., Kukkadapu, R. K., Eberl, D. D., Morton, J. P. and Kim, J., 2006. Microbial reduction of fe(III) in the Fithian and Muloorina illites: contrasting extents and rates of bioreduction. *Clays and Clay Minerals*, [e-journal] 54(1), pp.67–79. https://doi.org/10.1346/CCMN.2006.0540109.

Selim, K. A. and Rostom, M., 2018. Bioflocculation of (Iron oxide – Silica) system using *Bacillus cereus* bacteria isolated from Egyptian iron ore surface. *Egyptian Journal of Petroleum*, [e-journal] 27(2), pp.235–240. https://doi.org/10.1016/j.ejpe.2017.07.002.

Senoussi, H., Osmani, H., Courtois, C. and Bourahli, M. el H., 2016. Mineralogical and chemical characterization of DD3 kaolin from the east of Algeria. *Boletín de la Sociedad Española de Cerámica y Vidrio*, [e-journal] 55(3), pp.121–126. doi:https://doi.org/10.1016/j.bsecv.2015.12.001.

Štyriaková, I., Mockovčiaková, A., Štyriak, I., Kraus, I., Uhlík, P., Madejová, J. and Orolínová, Z., 2012. Bioleaching of clays and iron oxide coatings from quartz sands. *Applied Clay Science*, 61, pp.1-7.

Štyriaková, I. and Štyriak, I., 2000. Iron Removal from Kaolins by Bacterial Leaching. *Ceramics-Silikáty*, 44(4), pp.135–141.

Štyriaková, I., Štyriak, I. and Kušnierová, M., 1999. The release of sulphidic minerals from aluminosilicates by *Bacillus* strains. *Process Metallurgy*, [e-journal] pp.587–596. https://doi.org/10.1016/S1572-4409(99)80060-1.

Štyriaková, I., Štyriak, I. and Malachovský, P., 2007. Nutrients Enhancing the bacterial iron dissolution in the processing of feldspar raw materials. *Ceramics−Silikáty*, 51(4), pp.202-209.

Štyriaková, I., Štyriak, I., Malachovský, P. and Lovás, M., 2006. Biological, chemical and electromagnetic treatment of three types of feldspar raw materials. *Minerals Engineering*, 19, pp.348-354.

Štyriaková, I., Štyriak, I., Malachovský, P., Večera, Z. and Koloušek, D., 2007. Bacterial clay release and iron dissolution during the quality improvement of quartz sands. *Hydrometallurgy*, 89, pp.99-106.

Štyriaková, I., Štyriak, I., Nandakumar, M. P. and Mattiasson, B., 2003. Bacterial destruction of mica during bioleaching of kaolin and quartz sands by *Bacillus cereus*. *World Journal of Microbiology & Biotechnology*, 19, pp.583-590.

Štyriaková, I., Jablonovská, K., Mockovčiaková, A., Bekéniyová, A., Štyriak, I., Kraus, I., Osacký, M. and Lovás, M., 2010. Dissolution of iron from quartz sands by basin bioleaching under static *in-situ* conditions. *Hydrometallurgy*, 104, pp.443-447.

Tahli, L., 2008. Test of removal of iron minerals from kaolin using HGMS. *Indonesian Mining Journal*, 11(11), pp.18-23.

Tsuneda, S., Aikawa, H., Hayashi, H., Yuasa, A. and Hirata, A., 2003. Extracellular polymeric substances responsible for bacterial adhesion onto solid surface. *FEMS Microbiology Letters*, [e-journal] 223(2), pp.287–292. https://doi.org/10.1016/s0378-1097(03)00399-9.

Van der Marel, H. W. and Krohmer, P., 1969. O-H stretching vibrations in kaolinite, and related minerals. *Contributions to Mineralogy and Petrology*, 22(1), pp.73–82. doi:https://doi.org/10.1007/bf00388013.

Van der Marel, H. W. and Zwiers, J. H. L., 1959. OH stretching Bands of the kaolin minerals. *Silicates Ind.*, 24, pp.359-368.

Vu, B., Chen, M., Crawford, R. and Ivanova, E., 2009. Bacterial extracellular polysaccharides involved in biofilm formation. *Molecules*, [e-journal] 14(7), pp.2535–2554. https://doi.org/10.3390/molecules14072535.

Wang, J., Liao, R., Tao, L., Zhao, H., Zhai, R., Qin, W. and Qiu, G., 2017. A comprehensive utilization of silver-bearing solid wastes in chalcopyrite bioleaching. *Hydrometallurgy*, [e-journal] 169, pp.152-157.

Xue, H., Fan, Y., Fan, Y., Ma, X. and Yao, S., 2023. Study of structural transformation and chemical reactivity of kaolinite-based high ash slime during calcination. *Minerals*, [e-journal] 13(4), pp.466–466. doi:https://doi.org/10.3390/min13040466.

Yap, H. J., Yong, S. N., Cheah, W. Q., Chieng, S. and Kuan, S. H., 2020. Bioleaching of kaolin with *Bacillus Cereus*: Effect of bacteria source and concentration on iron removal. *Journal of Sustainability Science and Management*, [e-journal] 15(4), pp.91–99. http://dx.doi.org/10.46754/jssm.2020.06.009.

Yong, S. N., (to be published) Elucidation of iron reduction mechanisms in kaolin bioleaching by *Bacillus* species. Masters thesis. Universiti Tunku Abdul Rahman.

Yong, S. N., Lim, S., Ho, C. L., Chieng, S. and Kuan, S. H., 2022. Mechanisms of microbial-based iron reduction of clay minerals: Current understanding and latest developments. *Applied Clay Science*, [e-journal] 228, p.106653. https://doi.org/10.1016/j.clay.2022.106653

Zegeye, A., Yahaya, S., Fialips, C., White, M., Gray, N. and Manning D. A. C., 2013. Refinement of industrial kaolin by microbial removal of iron-bearing impurities. *Applied Clay Science*, [e-journal] 86, pp.47-53. https://doi.org/10.1016/j.clay.2013.08.041.

APPENDICES

Appendix A: Graphs

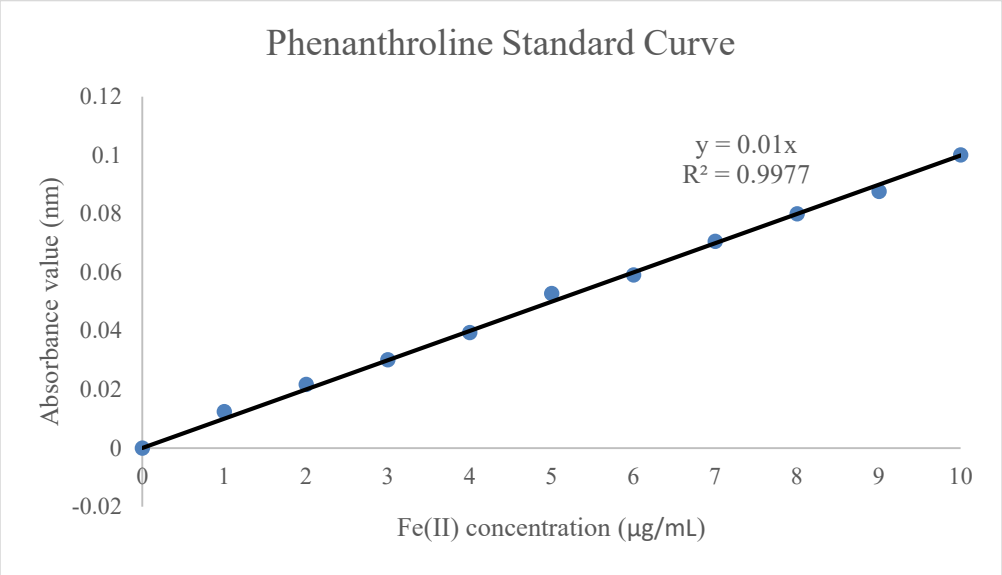

Graph A-1: Phenanthroline standard curve (Yong, n.d.).

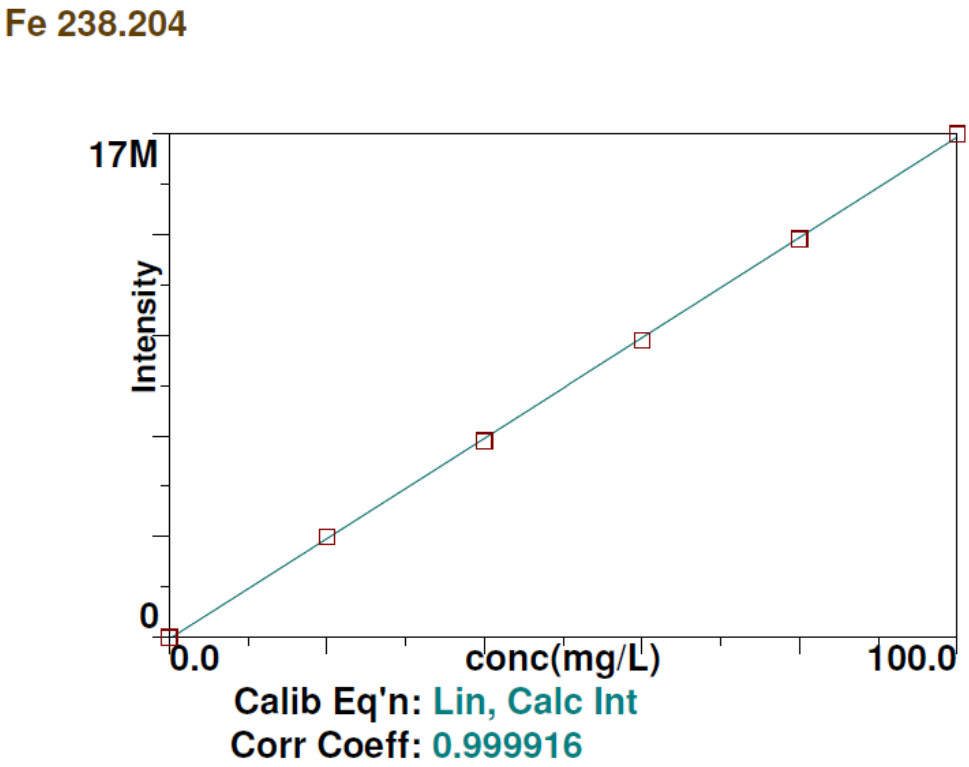

Graph A-2: Calibration curve of standard solution for ICP-OES.

Appendix B: Pictures

# Strongest 3 peaks no.	peak no.	2Theta (deg)	d (A)	I/I1	FWHM (deg)	Intensity (Counts)	Integrated Int (Counts)
1	12	24.9290	3.56894	100	0.26040	1135	16763
2	3	12.4051	7.12953	95	0.27550	1083	14538
3	20	38.4653	2.33846	26	0.38130	290	6206

Picture B-1: XRD analysis results strongest 3 peaks.

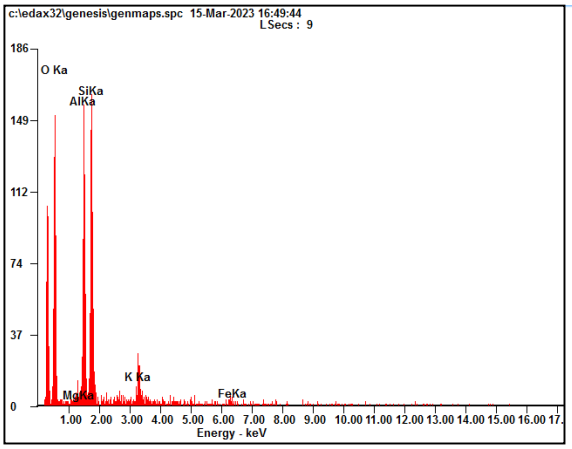

Element	Wt%	At%
OK	45.68	60.03
MgK	01.17	01.01
AlK	20.08	15.65
SiK	27.26	20.41
KK	04.40	02.37
FeK	01.41	00.53
Matrix	Correction	ZAF

Picture B-2: EDX results of raw Malaysian kaolin.

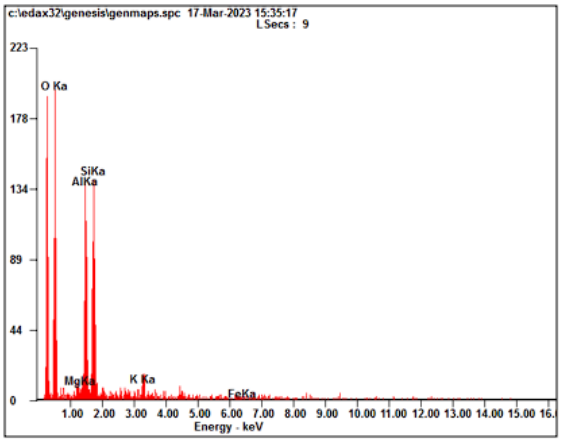

Element	Wt%	At%
OK	49.03	62.97
MgK	00.98	00.83
AlK	19.74	15.03
SiK	26.03	19.05
KK	03.62	01.90
FeK	00.60	00.22
Matrix	Correction	ZAF

Picture B-3: EDX results of Malaysian kaolin treated with *B. cereus*.

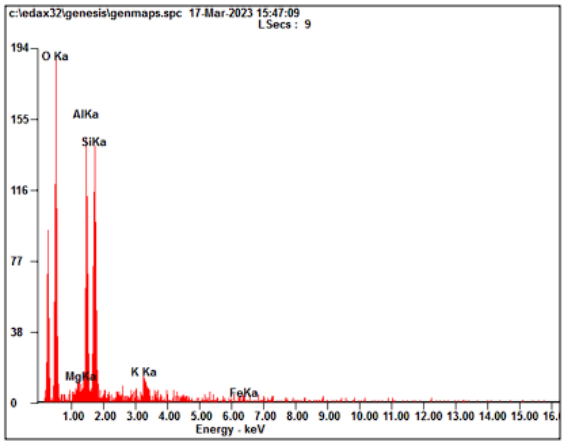

Element	Wt%	At%
OK	49.63	63.55
MgK	01.72	01.45
AlK	19.19	14.57
SiK	24.75	18.05
KK	04.15	02.17
FeK	00.56	00.21
Matrix	Correction	ZAF

Picture B-4: EDX results of Malaysian kaolin treated with *B. megaterium.*

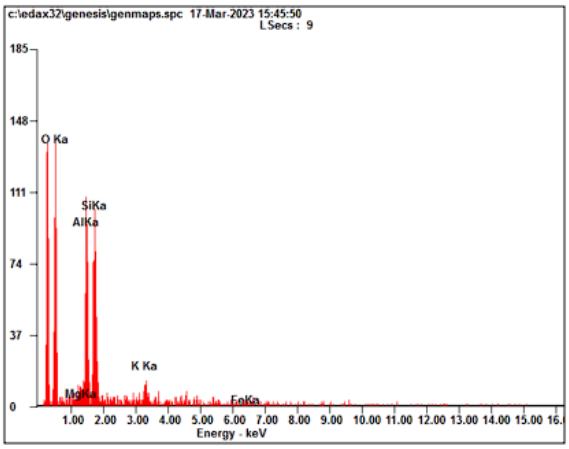

Element	Wt%	At%
OK	50.49	64.29
MgK	01.77	01.49
AlK	19.22	14.50
SiK	24.17	17.53
KK	03.87	02.02
FeK	00.48	00.17
Matrix	Correction	ZAF

Picture B-5: EDX results of Malaysian kaolin treated with *B. aryabhattai.*

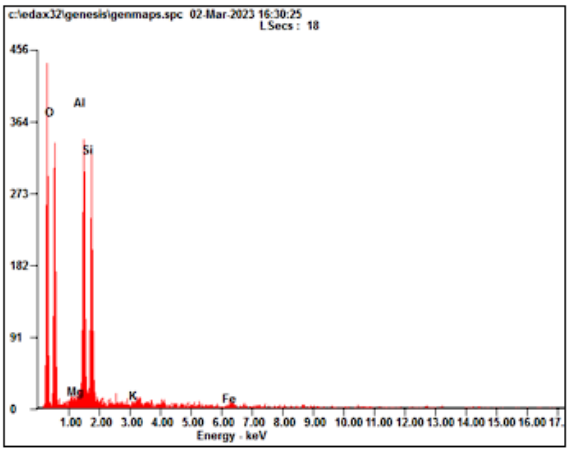

Element	Wt%	At%
OK	46.06	60.03
MgK	00.40	00.34
AlK	23.49	18.15
SiK	27.13	20.14
KK	01.55	00.83
FeK	01.37	00.51
Matrix	Correction	ZAF

Picture B-6: EDX results of raw Chinese kaolin.

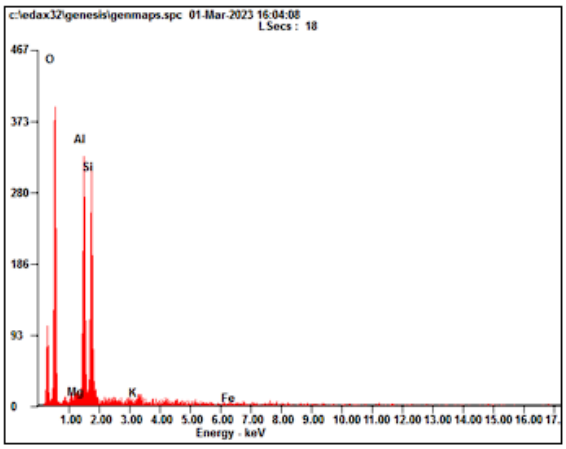

Element	Wt%	At%
OK	50.59	64.15
MgK	00.65	00.54
AlK	21.44	16.12
SiK	25.26	18.23
KK	01.26	00.65
FeK	00.80	00.30
Matrix	Correction	ZAF

Picture B-7: EDX results of Chinese kaolin treated with *B. cereus*.

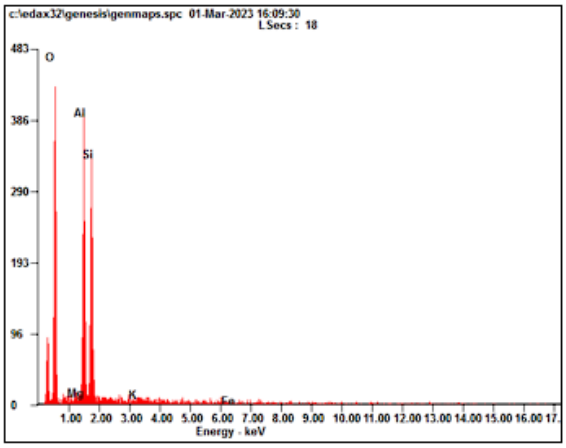

Element	Wt%	At%
OK	50.34	63.82
MgK	00.23	00.19
AlK	22.26	16.73
SiK	25.84	18.66
KK	00.71	00.37
FeK	00.62	00.23
Matrix	Correction	ZAF

Picture B-8: EDX results of Chinese kaolin treated with *B. megaterium*.

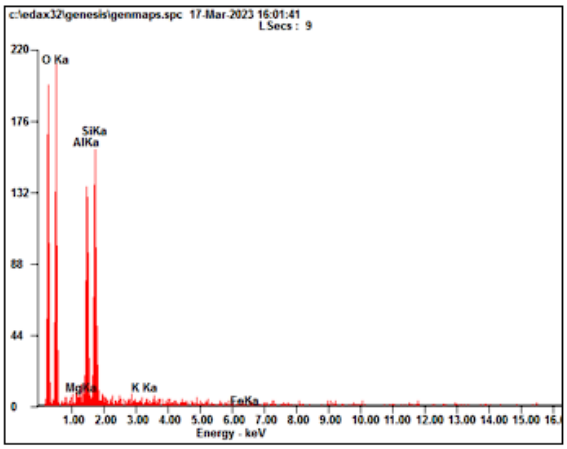

Element	Wt%	At%
OK	50.35	63.82
MgK	00.63	00.52
AlK	20.10	15.11
SiK	27.68	19.99
KK	00.73	00.38
FeK	00.51	00.19
Matrix	Correction	ZAF

Picture B-9: EDX results of Chinese kaolin treated with *B. aryabhattai*.

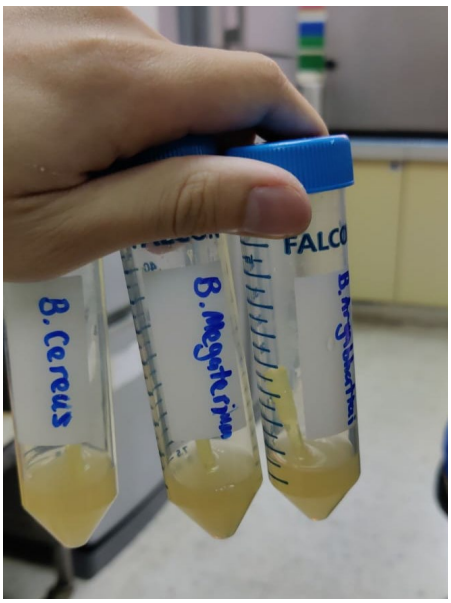

Picture B-10: Sub-culture of *B. cereus*, *B. megaterium*, *B. aryabhattai*.

Picture B-11: Magnetic stirrer (Thermolyne Cimarec).

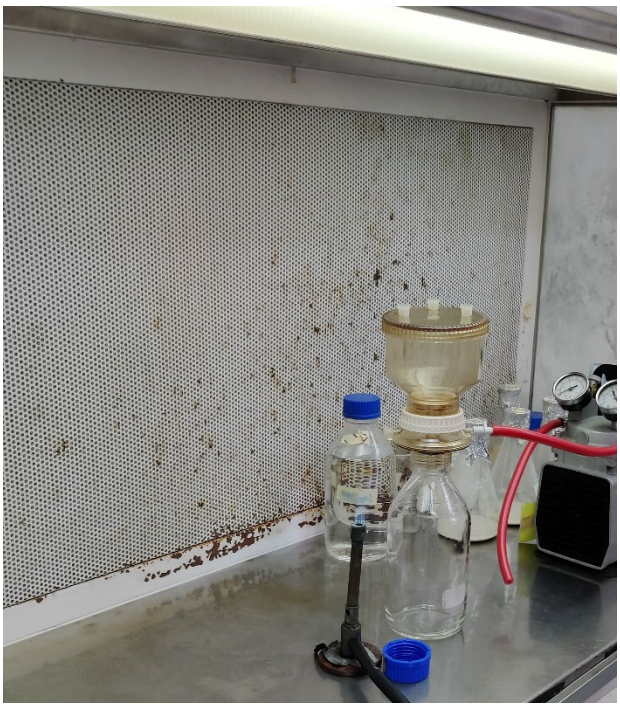

Picture B-12: Filter sterilization set up.

Picture B-13: Bioleaching of kaolin incubated at 30 °C 250 rpm.

Picture B- 14: Incubator (INFORS HT Ecotron) to incubate *Bacillus* bacteria at 37 °C 250 rpm.

Picture B-15: Filtration of bioleached samples.

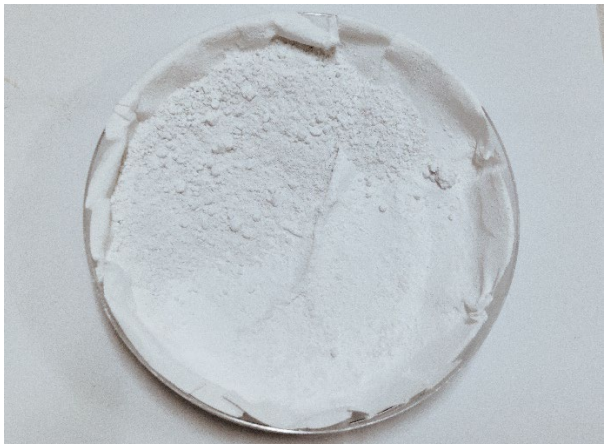

Picture B-16: Dried kaolin powder sample.

Picture B-17: Leftover residues from acid digestion.

Picture B-18: ICP-OES spectrometer (Perkin Elmer Optima 7000).

Picture B-19: Sample preparation for XRD.

Picture B-20: Shimadzu XRD machine (XRD6000).

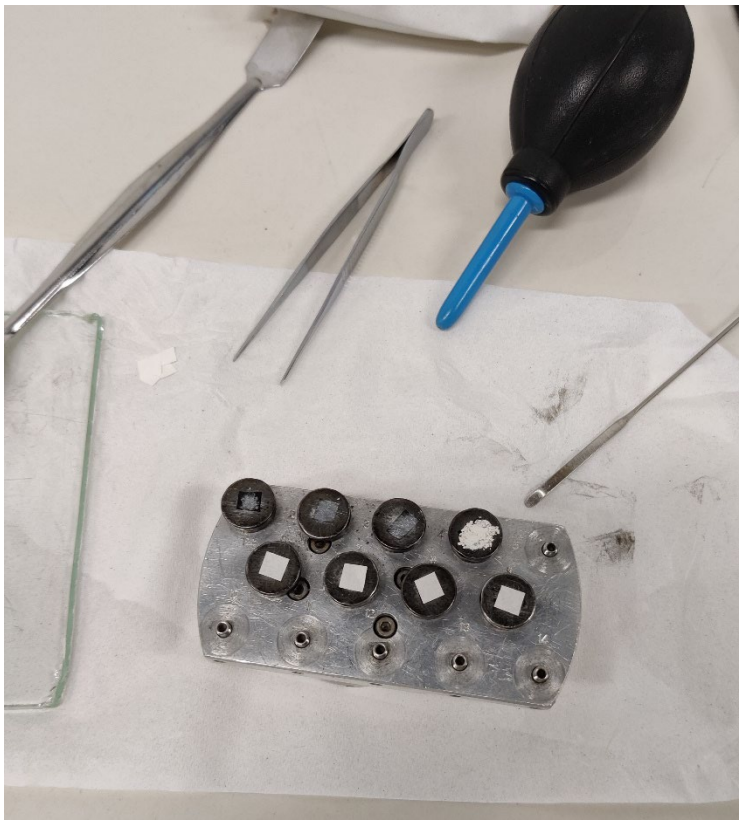

Picture B-21: Sample preparation for SEM-EDX.

Picture B-22: SEM-EDX (Hitachi, S-3400N).

Picture B-23: UV-VIS spectrophotometer (Nanodrop 2000c).

Picture B-24: Cell density meter (Ultrospec 10).

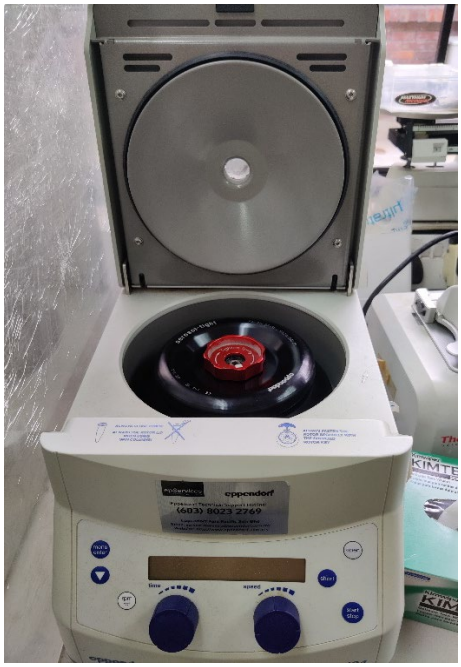

Picture B-25: Centrifuge (Eppendorf).

No.	Project Activities	Planned Completion Date	W1	W2	W3	W4	W5	W6	W7	W8	W9	W10	W11	W12	W13	W14	W15	W16	W17
1.	Register FYP title and understanding the FYP title.	2022-06-17																	
2.	Problem formulation and understanding of project objectives. Project planning with supervisor.	2022-07-01																	
3.	Analysis and research on Project by reading journals. Study on available bacteria for bioleaching of Kaolin Study the methods available to observe and analyze the morphological change in Kaolin.	2022-08-05																	
4.	Finish chapter 2, Literature Review and meet with supervisor for advice.	2022-08-05																	
5.	Generate methodology to propose the use of specified bacteria and method of studying the morphology of Kaolin.	2022-08-27																	
6.	Finalizing report writing	2022-09-10																	
7.	Report submission -FYP Report -Turnitin Report -Logbook -Presentation slides -Other relevant documents and Oral Presentation	2022-09-16																	
8.	Marked report review from supervisor and modify the progress report according to supervisor advice.	2022-09-30																	

Picture B-26: Project plan of FYP 1.

No.	Project Activities	Planned Completion Date	W1	W2	W3	W4	W5	W6	W7	W8	W9	W10	W11	W12	W13	W14	W15	W16	W17
1.	Revise Chapter 2 and 3. Conduct bioleaching experiment to determine the optimum nutrient condition through phenanthroline assay. Carry out the FTIR analysis on raw kaolin. Apply for approval for usage of lab to conduct SEM-EDX, XRD and ICP-OES.	2023-02-12																	
2.	Conduct bioleaching experiment based on the optimum nutrient (glucose) concentration. Collect the results on day 0, day 5 and day 10. Conduct phenanthroline analysis to determine the amount of iron(II) leached.	2023-02-27																	
3.	Study, observe and analyze the morphological change in kaolin through SEM-EDX, XRD and FTIR analysis. Prepare the sample for ICP-OES by using microwave digestor to acid digest the sample. Prepare standard solution for ICP-OES results.	2023-03-24																	
4.	Redo the experiment or analysis for any inconsistencies to get an accurate result.	2023-04-09																	
5.	Report writing and discussion of results. Finalize FYP report. Presentation slides preparation.	2023-04-30																	
6.	Submission of Final FYP Report. FYP Presentation. Revision of FYP report and resubmission.	2023-05-26																	

Picture B-27: Project plan of FYP 2.